Early Middle Triassic trace fossils from the Luoping Biota, southwest China: evidence of recovery from mass extinction

Mao Luo[a, b, c, *], G. R. Shi[a], Shixue Hu[d], Michael J. Benton[e], Zhong-Qiang Chen[b,**], Jinyuan Huang[d], Qiyue Zhang[d], Changyong Zhou[d], Wen Wen[d]

[a]*Deakin University, Geelong, Australia. School of Life and Environmental Sciences & Centre for Integrative Ecology, (Burwood Campus). 221 Burwood Highway, Burwood Victoria, 3125*

[b]*State Key Laboratory of Biogeology and Environmental Geology, China University of Geosciences, Wuhan 430074, China*

[c]*State Key Laboratory of Geological Processes and Mineral Resources, China University of Geosciences, Wuhan 430074, China*

[d]*Chengdu Centre of China Geological Survey, Chengdu 610081, China*

[e]*School of Earth Sciences, University of Bristol, Bristol, BS8 1RJ, UK*

**Email address: m.luo@deakin.edu.au (M. Luo), zhong.qiang.chen@cug.edu.cn (Z.Q. Chen)

Abstract

Trace fossils have proven useful for studying the timing and process of biotic recovery after the Permian–Triassic Mass Extinction (PTME). Recovery stages are defined by comparing successive ichnoassemblages from the latest Permian to the early Middle Triassic. Lower Triassic trace fossils have been explored in some detail, but those of the lower Middle Triassic are less well known. Here, well-preserved fossil materials from the Luoping Biota from Yunnan Province, South China suggest that a fully recovered shallow marine ecosystem was re-established by the early Middle Triassic. Trace fossil assemblages of the Luoping Biota are characterized by high ichnodiversity, with 14 ichnogenera in the shallow marine

environment of an intra-carbonate platform basin, and nine ichnogenera in the subtidal environment. Such moderate to high ichnodiversity, together with a marked increase in burrow sizes and the common occurrence of key ichnotaxa (e.g. *Rhizocorallium* and *Thalassinoides*) suggest that the ichnofauna had reached recovery stage four. In contrast, non turbiditic strata of the offshore setting record only three ichnogenera, with bioturbation indices never exceeding one. Periodic anoxia in bottom waters was presumably the main control for such a protracted trace fossil recovery in an offshore setting, which otherwise aided the fine preservation of body fossils of the Luoping Biota. Furthermore, event sedimentation (turbidite deposits) in the offshore setting incorporates moderate ichnodiversity and moderate to high bioturbation indices, both interpreted as a result of short-term colonization by transported infaunal animals from proximal settings. The occurrence of variable crustacean traces (e.g. *Sinusichnus*, *Spongeliomorpha*, and *Thalassinoides*) at Luoping and the locomotion traces of marine reptiles, together with abundant fishes and fossil decapods, highlights the value of trace fossils in ecosystem reconstruction after the PTME.

Keywords: biotic recovery, ichnological parameter, Guanling Formation, Yunnan, South China

1. Introduction

The Permian–Triassic Mass Extinction (PTME), with approximately 90% loss of marine invertebrate and ~ 80% of terrestrial vertebrate species, is considered the most severe in its ecological impact on both marine and continental ecosystems (Erwin et al., 2002; Erwin, 2006; McGhee et al., 2004). It was not until the early Middle Triassic that fully recovered shallow marine ecosystems were re-established (Chen and Benton, 2012). The PTME and subsequent recovery have been widely studied, with key questions regarding the extinction mechanism and recovery process remaining open for continued research (Chen and Benton, 2012; Foster and Twitchett, 2014).

Trace fossils have proven useful as a means of deciphering the timing and patterns of biotic recovery after the PTME (Twitchett and Wignall, 1996; Pruss and Bottjer, 2004; Twitchett, 2006; Chen et al., 2011, 2012; Hull and Darroch, 2013). Trace fossils provide invaluable information regarding biotic perturbations that is not readily available through

geochemical, sedimentological, and modelling-based studies (Morrow and Hasiotis, 2007; Zonneveld, 2011). Trace fossils represent the activities of both skeletonized and soft-bodied organisms. Soft-bodied organisms account for a large percentage of the total biomass within marine ecosystems (Allison and Briggs, 1991; Sperling, 2013), but are typically only preserved in the form of trace fossils. Hence, ichnofossils potentially provide more complete records of the behaviours of both infaunal and epifaunal organisms than do body fossils, thus facilitating the study of community structures and composition (Morrow and Hasiotis, 2007).

Lower Triassic trace fossils from all over the world have been studied extensively, yielding key data on the timing and process of recovery of trace-making organisms from the PTME (e.g. Twitchett and Wignall, 1996; Twitchett, 1999; Pruss and Bottjer, 2004; Twitchett and Barras, 2004; Beatty et al., 2008; Fraiser and Bottjer, 2009; Chen et al., 2011; 2012, 2015; Zonneveld et al., 2010; Knaust, 2010; Hofmann et al., 2011; 2015; Luo, 2014; Luo and Chen, 2014; Shi et al., 2015; Baucon and Carvalho, 2016; Luo et al., 2016; Feng et al., 2017a, b). Recovery stages were defined by comparing ichnological parameters of locally studied ichnoassemblages from the Early Triassic with those from the latest Permian and early Middle Triassic (e.g. Twitchett and Barras, 2004; Twitchett, 2006; Zonneveld et al., 2010; Pietsch and Bottjer, 2014). These comparisons suggest a step-wise recovery of trace-making organisms, as documented by the gradual increase in ichnodiversity, burrow size, tiering level, and the appearance of key ichnotaxa, from the Griesbachian to Spathian (Twitchett, 2006; Pietsch and Bottjer, 2014). Meanwhile, highly diverse ichnoassemblages discovered in the earliest Triassic suggest the presence of refugia in certain high-latitude regions and some potential equatorial regions, which facilitated a faster recovery of trace makers (e.g. Zonneveld et al., 2010; Knaust, 2010; Godbold et al., 2017).

Despite these intensive ichnological studies of Lower Triassic successions around the world, relatively little attention has been paid to trace fossils from the pre- and post-recovery intervals (Wignall et al., 1995, 1998; Zonneveld et al., 2001; Zhao et al., 2010; Ding et al., 2016; Uchman et al., 2016; Feng et al., 2017c), in order to better understand the timing and pattern of biotic recovery.

Recently, the lower Middle Triassic Guanling Formation from Luoping County in Yunnan province, Southwestern China has attracted substantial attention for the discovery of the Luoping Biota (Zhang et al., 2008a; 2009; Hu et al., 2011; Chen and Benton, 2012; Feldmann et al., 2012, 2015; Wen et al., 2012, 2013; Benton et al., 2013; Huang et al., 2013; Liu et al., 2014; Schweitzer et al., 2014; Zhang et al., 2014). Prolific vertebrate and invertebrate fossils from this biota record a well-developed shallow marine ecosystem in the middle–late Anisian,

suggested as marking the final stage of recovery after the PTME (Hu et al., 2011; Chen and Benton, 2012; Benton et al., 2013; Liu et al., 2014). Meanwhile, trace fossils (including coprolites) are similarly well preserved in association with body fossils in the Luoping Biota. They provide an extraordinary window into the behaviours of trace-making organisms from a stabilized, fully recovered shallow marine ecosystem after the PTME. Although some exceptionally preserved examples of coprolites and paddle imprints of nothosaurs from the Luoping Biota sites have been recently studied (Hu et al., 2011; Zhang et al., 2014; Luo et al., 2017), most of the burrowing traces remain unstudied.

Accordingly, this paper aims to document this trace fossil assemblage from the Luoping Biota, and compare it with those from Lower Triassic successions of South China and other regions of the world. The possibility of using the Luoping trace fossil records as a template to interpret the timing of recovery of trace-making organisms is also explored.

2. Geological setting, stratigraphy and depositional environment

2.1. Geological setting and stratigraphy

The three studied sections are located in Luoping County, eastern Yunnan Province, Southwest China (Fig. 1). During the early Middle Triassic, Luoping, together with its border areas between eastern Yunnan and western Guizhou Provinces, was located on the southwestern part of the Yangtze Platform and separated from the Nanpanjiang Basin by a shoal complex (Feng et al., 1997; Lehrmann et al., 2005; Enos et al., 2006; Fig. 1B). Within the vast Yangtze Platform interior, several spatially and temporally separated intraplatform basins or depressions with exceptional fossil preservation, namely the Panxian, Luoping, Xingyi, and Guanling, have been recognized from the late Anisian, late Ladinian and Carnian intervals, respectively (Hu et al., 2011; Benton et al., 2013). These basins shared similar features, including restricted circulation, density stratification of the water column, and dysoxic to anoxic bottom waters during the burial of these exceptionally preserved vertebrate faunas through various stages of the Triassic (Benton et al., 2013). At Luoping, abundant marine reptile faunas were preserved in a basinal setting represented by the upper part of Member II of the Guanling Formation (Hu et al., 2011). The highly fossiliferous, dark micritic limestone of the upper part of Member II can be traced over an area of around 200 km^2 (Benton et al., 2013). Member I and the lower–middle parts of Member II of the Guanling

Formation record similar successions over the entire Yangtze Platform interior region in the Yunnan-Guizhou border areas (Enos et al., 2006; Feng et al., 2017b, 2017c).

The Guanling Formation is subdivided into two members. Member I is dominated by siliciclastic sediments representing deposition in subtidal to intertidal environments (Hu et al., 1996), whereas Member II comprises micritic limestone, bioclastic limestone, oncoidal limestone and dolomite in the lower and middle parts, and black muddy limestone, cherty limestone, and grey dolomite in the upper part. Integration of sedimentary facies analysis, palaeontology and taphonomy indicates that the lower and middle parts of Member II were deposited in relatively open, shallow marine settings, whereas the upper portion of the member was deposited in a low-energy, semi-enclosed intraplatform basin influenced by episodic storms (Hu et al., 2011). The Guanling Formation in the Luoping area, overall, records a progressively deepening succession (Zhang et al., 2008a).

The *Nicoraella kockeli* Conodont Zone has been detected in the upper part of Member II. This conodont zone includes elements, such as *Nicoraella germanicus*, *Nicoraella kockeli* and *Cratognathodus* sp., indicative of the Pelsonian age of the middle Anisian (Zhang et al., 2009). The underlying Member I of the Guanling Formation yields the bivalves *Myophoria* (*Costatoria*) *goldfussi mansuyi* Hsü, *Unionites spicatus* Chen, *Posidonia* cf. *pannonica* Moj, and *Natiria costata* (Münster), and contains several clay beds. This bivalve assemblage is of early Anisian age in South China (Zhang et al., 2008a), and the clay beds have been regarded as correlation markers for the base of the Anisian in southwest China (Enos et al., 2006; Zhang et al., 2009).

2.2. Interpretation of depositional environment

Three sections have been excavated systematically at Luoping for fossil collection and study of the stratigraphy and depositional environment. They are named Dawazi (or Daaozi) (DWZ), Shangshikan (SSK), and Xiangdongpo (XDP), respectively (Zhang et al., 2008a; 2009; Huang et al., 2009; Bai et al., 2011; Hu et al., 2011; Figs. 1A, 2). The Middle Triassic successions in these three excavation sites correlate well with each other by a sharply based, bioturbated wackestone separating the upper and lower fossiliferous units (Bai et al., 2011; Zhang et al., 2014). Further, the three sections are located close together, and individual limestone marker beds can be traced across country between the sections. The thickly bedded

limestone unit bears extremely consistent features, including thorough bioturbation, the inclusion of burrows filled by silica concretions, and almost uniform thickness, thus serving as a clear marker unit. Following this recognition, three stratigraphic units have been defined and correlated in the three sections. The documented sedimentary features of these units and their environmental interpretations are as below.

2.2.1. Unit A (shallow to deep subtidal)

Unit A is composed of medium-to thick-bedded bioclastic wackestone and oncoidal pack-wackestone with a small proportion of calcareous mudstone (Fig. 3A, G, H). In DWZ and SSK, stromatolitic bindstones also occur as major constituents. Fragmented bivalve shells, echinoderms, and ostracods are the main skeletal components in wackestone and packstone, with faecal pellets as subordinate grain types. Planar lamination is well developed in both wackestone and carbonate mudstone facies, with bioturbation index (BI) ranging from 1 to 4 (BI schemes follow Reineck, 1963, and Taylor and Goldring, 1993). BI 1 represents sparse disruption of sediments (1–4%) whereas BI 4 is characterized by intense bioturbation (61–90%). Wavy crinkled lamination developed locally in the dolomitic limestone (Fig. 3H)

The dominance of muddy facies in this association indicates a deep subtidal setting. Oncoids indicate moderate energy conditions in shallow water. Stromatolitic build-ups have been observed from shallow to deep subtidal environments in the Triassic (e.g. Flügel et al., 2004, p. 57; Ezaki et al., 2008, 2012). Thus, a shallow to deep subtidal setting is interpreted for Unit A.

2.2.2. Unit B (offshore)

Unit B is composed mainly of very thin bedded (1–3 cm) marly carbonate mudstones intercalated with very thin-bedded (1 cm) black shales (Fig. 3B–C), bioturbated wackestones, and minor thin-bedded packstones. Thin bedded to lenticular chert layers and cherty nodules are also prominent. Planar lamination and reticulated ridge structures (Fig. 3B–C; Luo et al., 2013) are pervasively developed in marly carbonate mudstones, followed by locally occurring convolute lamination. Disseminated pyrite crystals and pyrite framboids are common in marly carbonate mudstones (Fig. 8A, C), in which bioturbation is absent except for a few surficial trails preserved on bedding planes. Locally, normally graded packstone beds have a basal sharp and erosive contact, which are overlain by planar to convolute lamination and massive

carbonate mudstones (Fig. 3D). These coarse-grained beds are also characterized by pervasive bioturbation. Thick-bedded, sharp-based nodular (bioturbated) wackestone marker layers separate the upper and lower marly carbonate mudstone beds/units (Fig. 3E), in which abundant well-preserved vertebrate and invertebrate fossils have been discovered, respectively (Fig. 2; Bai et al., 2011; Benton et al., 2013; Zhang et al., 2014; Luo et al., 2017). Several ash layers also occur intercalated in the marly carbonate mudstones of Unit B (Fig. 2).

The overall fine-grained sediments of Unit B are interpreted as deposits from suspension in a low-energy environment with weak current activity. This is shown by the thinly laminated nature of the marly carbonate mudstones and shales. Reticulated ridge structures have been interpreted as indications of benthic microbial mats (Luo et al., 2013). The wide occurrence of benthic microbial mats required a water depth within the photic zone, the lower limit of which is 80–100 m (e.g. James and Bourque, 1992, p. 326). The packstone beds, with their overlain planar/convolute-laminated sediments and massive carbonate mudstones represent Ta, Tb and Te of the Bouma Sequence, which are interpreted to be the result of low-density, dilute turbiditic currents (e.g. Walker, 1992). Similar thin-bedded turbidite deposits have also been observed in the Meride Limestone of the Monte San Giorgio Lagerstätte (Stockar, 2010). Furthermore, turbidite current activity is further supported by the bedded nature of the chert beds, which is interpreted as the result of rapid, turbiditic input of biogenic sediments (e.g. McBride and Folk, 1979; Bustillo and Ruiz-Ortiz, 1987). The common occurrence of pyrite framboids in the carbonate mudstones possibly indicates anoxic bottom water conditions. To sum up, Unit B represents deposition in an anoxic offshore environment.

2.2.3. Unit C (offshore transition)

Unit C is composed of thin- to medium-bedded hummocky cross-stratified wackestones (Fig. 3F), carbonate mudstones, with minor intraclastic floatstones and bioclastic packstones. Wackestone beds are sharply to erosively based, with a few cherty nodules present locally. Convolute lamination and gutter casts also occur. Bioturbation is pervasive in the wackestones and carbonate mudstones. Intraclasts are composed of carbonate mudstone. Packstone layers are lenticular and have graded bedding in the basal parts.

Packstones with a graded basal part, together with their lenticular morphology are most likely associated with storms. Such storm activity is also indicated by the frequent occurrence of hummocky cross-stratification, which is interpreted as a combination of waning oscillatory flow and unidirectional currents created by periodic storm events (Dott and Bourgeois, 1982;

Dumas and Arnott, 2006). Thus, Unit C is interpreted as the deposits of an offshore transitional environment.

3. Ichnological features of the Luoping Biota

Fourteen ichnotaxa have been identified from the three studied sections through Member II of the Guanling Formation. These ichnotaxa are distributed in both the lower and upper fossil layers and strata above and below (Fig. 2). Detailed descriptions of all discovered trace fossils and ichnological parameters are presented below.

3.1. Ichnological descriptions

3.1. Archaeonassa *Fenton and Fenton, 1937*

3.1.1. Archaeonassa fossulata *Fenton and Fenton, 1937 (Fig. 4A)*

Preserved as concave epirelief on upper bedding plane of carbonate mudstone. Grooved trails are gently curved, and are flanked by rounded ridges. Width of trail is about 10 mm and length up to 230 mm. Width remains consistent in individual trails.

Remarks: The grooved trail flanked on both sides by rounded ridges is diagnostic of *Archaeonassa* (Fig. 4A). Although the observed specimen from the DWZ section is similar to *Helminthopsis*, the meandering characteristics of *Helminthopsis* are more complicated than those of *Archaeonassa*. *Archaeonassa* is typically preserved in intertidal regimes where such traces may be abundant (Fenton and Fenton, 1937), and it may also occur more rarely in shallow marine environments. *Archaeonassa* is also known from continental environments (e.g. Buckman, 1994; Buatois and Mángano, 2002). *Archaeonassa* can be produced by various invertebrates, including molluscs and arthropods (Buckman, 1994; Yochelson and Fedonkin, 1997).

3.2. Arenicolites *Salter, 1857*

3.2.1. Arenicolites isp. *(Fig. 4B)*

Preserved as paired tubes on upper bedding planes of carbonate mudstones and wackestones. Tubes are preserved as hollow, funnel-shaped openings with no burrow fill or probably eroded away. Tube diameters range from 7 to 18 mm and the distance between the tubes (width) is up to 62 mm. Diameters of the two tubes in a pair are slightly different.

Remarks: *Arenicolites* and *Skolithos* are difficult to distinguish when they occur densely on bedding planes. The tube structures are usually paired, justifying a reasonable assignment to *Arenicolites*. No spreiten structures have ever been observed between the paired tubes, excluding their assignment to *Diplocraterion*. *Arenicolites* is regarded as an element of the shallow marine *Skolithos* ichnofacies and firmground *Glossifungites* ichnofacies (e.g. Buatois and Mángano et al., 2011a; MacEachern et al., 2012), although such biogenic structures also occur in freshwater deposits (Bromley and Asgaard, 1979). Trace producers include various worm-like organisms, such as polychaetes (Bradshaw, 2010).

3.3. Dikoposichnus *Zhang et al., 2014*

3.3.1. Dikoposichnus luopingensis *Zhang et al., 2014 (Fig. 4C)*

Large, narrow V-shaped slot-like depressions preserved as single or paired imprints on both upper bedding plane (concave epireliefs) and sole surfaces (convex hyporeliefs). Individual imprint is elliptical to sigmoidal, with an anterior sweep at the medial edge. Paired imprints commonly consist of long (up to 18.7 m) trackways that are 30–70 cm wide.

Remarks: This new trace was introduced by Zhang et al. (2014) based on materials from bed 107 of the DWZ section. The well-preserved footprints in long trackways are paired, suggesting the limbs moved in concert. They were interpreted as the paddle imprints of a limbed vertebrate (e.g. nothosaur) moving in a steady manner over the seabed searching for prey (Zhang et al., 2014). It is considered to represent the first locomotion record of marine reptiles from the Mesozoic.

3.4. Diplocraterion *Torell, 1870*

3.4.1. Diplocraterion isp. *(Fig. 4D–F)*

Paired tubes with variable size ranges in both burrow width and diameter. Maximum burrow diameter can reach 17.5 mm and width of up to 84 mm. There are very delicately

preserved spreiten structures within shafts connecting the two tubes. Burrow fill of tubes and connected shafts have a darker colour than the host rock.

Remarks: In plan view, the dumbbell-shaped structure, in which the paired tubes are linked by spreiten, justifies assignment to *Diplocraterion*. There is no further evidence of detailed structures in vertical profiles, which prevents assignment to an ichnospecies. Features of the spreiten that connect the paired tubes suggest it is protrusive, indicating a downward movement of trace makers in response to possible erosion of the sediment surface (Bromley, 1996; Buatois and Mángano, 2011a). Dense preservation of these burrows as patch assemblages indicates some possible opportunistic strategies of the trace makers (e.g. Vossler and Pemberton, 1988). In particular, variably sized *Diplocraterion* occurring together could be the product of different generations of animals. *Diplocraterion* is regarded as a dwelling trace of suspension feeders and has a stratigraphic range from Cambrian to present (Abbassi, 2007). It is a characteristic member of the *Skolithos* ichnofacies, and also the substrate-controlled *Glossifungites* ichnofacies (MacEachern et al., 2007; Buatois and Mángano, 2011a). It has also been utilized for defining sequence boundaries and stratigraphic correlation (Taylor and Gawthorpe, 1993; Olóriz and Rodríguez-Tovar, 2000).

3.5. Megagrapton *Książkiewicz, 1968*

3.5.1. Megagrapton irregulare *Książkiewicz, 1968 (Fig. 4G)*

Cord-sized strings preserved as convex hyporeliefs; burrows meander irregularly and branching at right angles. Meandering burrows also form irregular, rectangular meshes that are not closed.

Remarks: The specimen observed at Luoping has diagnostic features including perpendicular branching angles and unclosed meshes resembling *Megagrapton irregulare*. *Megagrapton* is a typical ichnotaxon of flysch strata, usually preserved on sole surfaces in association with other graphoglyptids. It bears some characteristics resembling *Protopaleodictyon* (Książkiewicz, 1977; Uchman, 1998). *Megagrapton* has been commonly observed in Permian to Cretaceous flysch strata in China (e.g. Zhang et al., 2008b).

3.6. Palaeophycus *Hall, 1847*

337 *3.6.1.* Palaeophycus isp. *(Fig. 5A)*

338 Simple, horizontal to inclined cylindrical burrows preserved in carbonate mudstones.
339 Burrows are straight to slightly curved, sub-circular in cross-section. The burrow wall is
340 smooth, and burrow width ranges from 8 to 13 mm. Burrow linings are typical. Burrow fill is
341 the same in colour and composition as the host rock.

342

343 *Remarks:* The similarity of the burrow fill and the surrounding host rock and burrow
344 lining are typical of the ichnogenus *Palaeophycus* (e.g. Osgood, 1970; Pemberton and Frey,
345 1982). *Palaeophycus* is a facies-crossing ichnogenus and occurs from the Precambrian to
346 present (Pemberton and Frey, 1982).

347

348 *3.7.* Planolites *Nicholson, 1873*

349

350 *3.7.1.* Planolites isp. (Fig. 5B)

351 Horizontal, smooth trails that are straight to gently curved. They are circular to elliptical
352 in transverse section. Burrows are unbranched, and commonly cross-cut each other. Burrow
353 fill is structureless, and is darker than the host rock. Burrow diameters range from 2.1 to 25.1
354 mm, and average 10.5 mm.

355

356 *Remarks:* The unlined burrow and its darker colour in contrast to the host rock is
357 diagnostic of *Planolites*. It is a facies-crossing ichnotaxon, ranging through a wide variety of
358 environments from shallow to deep marine and also nonmarine. Its producer includes certain
359 vermiform deposit feeders (e.g. Pemberton and Frey, 1982; Uchman, 1995). *Planolites* also
360 has a wide stratigraphic range from the Precambrian to present (Häntzschel, 1975).

361

362 *3.8.* Rhizocorallium *Zenker, 1836*

363

364 *3.8.1.* Rhizocorallium isp. *(Fig. 5C)*

365

366 Gently inclined to horizontal, U-shaped tubes are preserved as full reliefs in carbonate
367 mudstones/wackestones. U-tube has dark burrow fill in contrast to the host rock (Fig. 5C). No
368 spreiten structures are evident between limbed tubes. Burrow size (width of U tube) ranges
369 from 16 to 43 mm, with an average value of 26.1 mm (Fig. 7C). Clustered individuals cross

cut-each. They are also found to cross-cut the previously formed, meshwork burrowing systems resembling *Thalassinoides*.

Remarks: Specimens from the Guanling Formation in the Luoping area bear certain characteristics resembling *Rhizocorallium commune* (Knaust, 2013). These include their gregarious nature, the relatively smaller size compared with *R. jenense* (see below), and their cross-cutting relationships. However, the absence of scratches along marginal tubes prevents unequivocal assignment. *Rhizocorallium* can be produced by various animals including decapods, crustaceans, annelids, polychaetes, and also mayflies (Knaust, 2013).

3.8.2. Rhizocorallium jenense *Zenker, 1836 (Fig. 5D–F)*

These U-shaped burrows are isolated, and preserved as horizontal epirelief or hyporeliefs. Burrow fill has similar colour to the host rock. Typical spreiten structures between the limbed tubes are characteristic (Fig. 5D–E). The whole U-shaped tubes form long tongue-shaped structures and even complex spiral burrowing systems. Ornamented faecal pellets are evident in limbed burrows (Fig. 5F). Burrow width of U-tubes ranges from 27 to 74.5 mm, and averages 51.3 mm (Fig. 7B).

Remarks: These specimens are assignable to *Rhizocorallium jenense*, which is characterized by an elongate morphology, larger size and prominent faecal pellets in limbed tubes. *Rhizocorallium* is an element of the *Cruziana* ichnofacies and also a representative ichnotaxon of the firmground *Glossifungites* ichnofacies (Buatois and Mángano, 2011a). *Rhizocorallium* has been widely recognized in strata from the lower Cambrian to Cenozoic (e.g. Knaust, 2013). The potential producer of *R. jenense* could be a polychaete (Knaust, 2013).

3.9. Sinusichnus *Gibert, 1996*

3.9.1. Sinusichnus isp. *(Fig. 5G–H)*

This trace is preserved as positive or negative hyporeliefs, and can be found over areas spanning several square decimetres. Horizontal burrows are knobbly, and show regular sinuous tunnels, but less regular to straight tunnels are also evident/present in the same branching system (Fig.5G). Branching points usually comprise three points forming a Y- or T-shaped junction (Fig. 5G). In some cases, two closely emplaced triple junctions form an H-like configuration. Four-pointed branching is also apparent locally. The burrow system

penetrates into the sediment at very shallow depths (no more than 1.5 cm). Retrusive spreiten were not observed. Diameters of sinuous burrows remain identical in each distinct burrow system, but vary slightly between different specimens. Measurements of 102 specimens reveal a burrow width ranging from 4 to 16 mm, with an average value of 8.8 mm.

Remarks: The newly discovered traces are extremely similar to the ichnogenus *Sinusichnus* established by Gibert (1996). This is revealed by the regular sinuous and branching morphology of the horizontal tunnels. In addition, the significant relationship between wavelength (λ) and amplitude (A) in the Luoping specimens has also been found in typical *S.sinuosus* (Gibert et al., 1999a). Apart from the type ichnospecies *S. sinuosus* established by Gibert (1996), Kapper (2003) proposed another ichnospecies, *S. priesti*, based on specimens from Upper Cretaceous strata in Germany. The only feature distinguishing *S. sinuosus* from *S. priesti* is the presence of bioglyphs in the latter. No scratch marks or bioglyphs are evident on the branching burrows observed herein. In addition, the knobbly appearance of the specimen suggests some lining of the burrows, a feature that is not present in *Sinusichnus*. It is noted also that the specimens studied here are less regular in some parts of the burrow segments compared with those from Pliocene and Miocene strata (e.g. Buatois et al., 2009; Belaüstegui et al., 2014). These features make it difficult to assign the specimen to any of the ichnospecies established. The trace *Sinusichnus* can be produced by decapod crustaceans and isopods, and has a stratigraphical range from Middle Triassic to Pliocene (e.g. Gibert, 1996; Buatois et al., 2009; Belaüstegui et al., 2014; Knaust et al., 2016).

3.10. Spongeliomorpha *Saporta 1887*

3.10.1. Spongeliomorpha isp. *(Fig. 6A)*

This trace is preserved as full relief on the upper surface of carbonate mudstones. Burrows exhibit Y-shaped branching, with delicate, longitudinal scratch marks seen on burrow wall surface. There is enlargement at burrow intersection. Burrow diameter ranges from 21 to 27 mm.

Remarks: The observed specimens bear characteristics, such as Y-shaped branching and scratched burrow walls, typical of *Spongeliomorpha*. However, it should be noted that the longitudinal striae (scratch marks) are different from the transversely oriented striations

reported in some previous work (e.g. Bromley and Asgaard, 1979), nor are they comparable with those observed in *S. iberica* (e.g. Melchor et al., 2009). An assignment at ichnospecies level is unresolved. Although several animals have been proposed as the possible trace makers of *Spongeliomorpha*, the enlargement at the bifurcating junction, together with scratch marks on the burrow wall surface, indicate that a decapod is most likely the trace maker for *Spongeliomorpha* isp. at Luoping. This trace has been found in both marine and nonmarine environments, and has a stratigraphical range from Early Permian to Miocene (Bromley and Asgaard, 1979; Carmona et al., 2004; Melchor et al., 2009).

3.11. Taenidium *Heer 1877*

3.11.1. Taenidium barretti *Bradshaw, 1981 (Fig. 6B)*

Unlined cylindrical burrow preserved in carbonate wackestone. In vertical profile, sinuous burrows contain dark, articulated burrow fill alternating with light meniscate partings. The alternating two types of sediment have varying thickness and are unevenly spaced. Burrow is unbranched, and has a consistent diameter of 10 mm.

Remarks: The specimen has a striking resemblance to *Beaconites antarcticus* as illustrated by Graham and Pollard (1982). However, following the reclassification of *Beaconites*, *Taenidium* and *Ancorichnu*s (Keighley and Pickerill, 1994), this trace fossil should be renamed as *Taenidium barretti*. The taxonomy of meniscate burrows was comprehensively reviewed and revised by D'Alessandro and Bromley (1987). Three ichnospecies were proposed as valid for *Taenidium* before *Taenidium barretti*, namely *T. serpentinum, T. cameronensis, and T. satanassi* (D'Alessandro and Bromley, 1987). The unbranched, meniscate structures observed herein have very gentle curvature, and consist of unevenly distributed dark and light menisci that are deeply arcuate and tightly packed. These features justify assignment to *Taenidium barretti*. *Taenidium* has been reported from strata ranging from the Cambrian to Eocene (D'Alessandro et al., 1986; D'Alessandro and Bromley, 1987; Yang et al., 2004), but most occurrences are from the Silurian–Devonian, and the Cretaceous to Eocene (e.g. Häntzschel, 1975, p.W84; Bradshaw, 1981).

3.12. Thalassinoides *Ehrenberg, 1944*

3.12.1. Thalassinoides suevicus *Rieth, 1932 (Fig. 6C)*

The burrows are preserved as either concave epirelief or convex hyporelief on carbonate mudstones/wackestones. Burrows typically occur as Y-shaped branching systems and have swollen bumps at conjunction points (Fig. 6C). Burrow surface is smooth. Burrow sizes range from 5 to 30 mm, and average 17.9 mm. Burrow shafts usually form complicated meshworks covering a maximum area of up to tens of square metres. Burrow penetration depth is shallow (no more than 5 cm). On some horizons of the XDP section, larger Y-shaped burrows systems were cross-cut by U-shaped *Rhizocorallium* isp.

Remarks: This trace is characterized by its Y-shaped branching. The swollen part at the junctions implies that these *Thalassinoides* traces were produced by decapod crustaceans (Bromley and Frey, 1974; Carmona et al., 2004; Carvalho et al., 2007). Such a trace fossil is usually interpreted as a dwelling or feeding structure produced by detritus-feeding crustaceans in shallow to deep marine environments (Myrow, 1995; Carvalho et al., 2007). Besides, *Thalassinoides* burrows are also present in the firmgound substrate of the *Glossifungites* ichnofacies immediately after the end-Permian crisis (Chen et al., 2015). *Thalassinoides* has a stratigraphical range from Cambrian to present (Myrow, 1995), but a decapod origin of such traces has been suggested for Devonian examples (e.g. Carmona et al., 2004).

3.13. Undichna *Anderson, 1976*

3.13.1. Undichna unisulca *Gibert et al., 1999 (Fig. 6D)*

These are unpaired sinuous ridges on sole surfaces of bedding planes of wackestones/packstones. Two single trails were identified, which are preserved as regular sinusoidal strings with equal wavelength and amplitude. The sinuous trail is composed of two to three ridges separated by subtle grooves.

Remarks: The Luoping specimens of single-waved trails are extremely similar to *Undichna unisulca* diagnosed by Gibert et al. (1999b) and Morrissey et al. (2004) in both morphology and preservation, and thus justify assignment to this ichnospecies. This trace has been interpreted to be generated by a fish swimming with its caudal fin in contact with the substrate (Gibert et al, 1999b). As fishes diversified from the Ordovician onwards, their behavioural product, *Undichna* also has a very wide stratigraphic distribution in the

505 Palaeozoic, Mesozoic and Cenozoic (Gibert et al., 1999b., Gibert, 2001; Benner et al., 2009;
506 Fillmore et al., 2011).
507
508
509 *3.14.* Zoophycos *Massalongo, 1855*
510
511 *3.1.14.* Zoophycos isp.? *(Fig. 6E, F)*
512 These are spiral-shaped structures composed of U-shaped protrusive, primary laminae of
513 variable orientation. Primary laminae arrange in helicoid spirals to form an overall elliptical
514 shape, with no marginal tubes observed.
515
516 *Remarks:* The primary laminae forming helicoid spirals is characteristic of *Zoophycos*
517 (e.g. Uchman, 1995), but the incomplete preservation of the specimen and absence of
518 marginal tubes prevent assignment to an ichnospecies. The origin of *Zoophycos* is unresolved,
519 although it is generally assumed to have been made by deposit-feeding organisms (Uchman,
520 1995; 1998), with sipunculoids, polychaete annelids, and enteropneust hemichordates all
521 possible trace makers (e.g. Wetzel and Werner, 1981; Ekdale and Lewis, 1991; Kotake, 1992).
522 *Zoophycos* has a stratigraphic age range from Cambrian to present (e.g. Zhang et al., 2015),
523 and its trace maker transferred from shallow water environments in the Palaeozoic to deep
524 marine environments since the Cretaceous (e.g. Seilacher, 1974; Zhang et al., 2015).
525
526
527 **4. Eco-ichnological characteristics**
528
529 *4.1. Abundance and ichnodiversity*
530
531 Fourteen ichnogenera were recorded from the three studied sections at Luoping. Among
532 these, six ichnogenera are more abundant than the others, and these form dense assemblages
533 at particular horizons. These are *Arenicolites*, *Dikoposichnus*, *Diplocraterion*, *Planolites*,
534 *Rhizocorallium*, and *Thalassinoides*. Other traces are only locally developed.
535 The offshore setting of Unit B is characterized by very low ichnodiversity and low BI. Non-
536 turbiditic strata, as represented by marly carbonate mudstone and shales are nearly devoid of
537 bioturbation, with only *Dikoposichnus*, *Megagrapton* and *Undichna* preserved as surficial
538 trails/tracks on bedding planes. It is the same case for both the upper and lower ‘fossil

horizons'. The sharply to erosively based turbidite beds, in contrast, have a moderate to high BI and a moderately diverse ichnoassemblage. Ichnotaxa in those event beds include *Diplocraterion, Planolites, Rhizocorallium, Sinusichnus, Taenidium,* and *Thalassinoides*. There is a marked increase in BI for the offshore transition of Unit C. Most of the beds were variously bioturbated, with BI ranging from two to four. However, the ichnodiversity remains low. Unit A saw the highest level of both BI and ichnodiversity. Nine ichnogenera were discovered from this unit, including *Archaeonassa*, *Arenicolites*, *Palaeophycus*, *Planolites*, *Sinusichnus*, *Rhizocorallium, Spongeliomorpha, Thalassinoides*, and ? *Zoophycos*. BI levels also increased, from one to four.

4.2. Burrow size

Burrow sizes of the abundantly preserved traces of the Luoping Biota were analyzed statistically. Burrow forms analyzed include *Diplocraterion*, *Planolites*, *Rhizocorallium* and *Thalassinoides* (Fig. 7A–D).

The average burrow width of *Diplocraterion* is 26.4 mm based on measurements of 135 individuals. *Planolites* has a wide range of burrow diameters (2.1–25.1 mm), average 10.5 mm (Fig. 7A). Two ichnospecies of *Rhizocorallium* were measured separately. For the larger group, burrow width of the U-tubes averages 51.3 mm (Fig. 7B), whereas the average width for the smaller one is 26.1 mm. For the mazework of *Thalassinoides*, the burrow widths range from 5 to 30 mm, with a mean value of 17.9 mm, based on 104 measurements (Fig. 7D).

4.3. Tiering level and complexity

Tiering level is practically evaluated by measuring the penetration depth of trace fossils, to explore ecospace utilization of sediment. Trace fossils are preserved at very shallow depths in marly carbonate mudstones of Unit B, where trails, such as *Megagrapton*, *Undichna* and *Dikoposichnus*, occupied only the upper 1–2 cm of the sediments. Vertical burrows, such as *Diplocraterion* and *Arenicolites*, also penetrate to depths of no more than 3 cm. Trace fossils in Unit C also have very shallow penetration depths. Those complex traces such as *Rhizocorallium*, *Spongeliomorpha* and *Thalassinoides*, occupied only the surficial 2–4 cm of the sediments.

Turbidite deposits in Unit B, on the other hand, have deeper burrows than their surrounding non-turbiditic sediments. Vertically oriented *Taenidium* has a penetration depth

of 5 cm. The silicified *Thalassinoides* burrows in marked horizons have an even deeper penetration depth up to 10 cm.

5. Discussion

5.1. Decoupled features between trace fossils and body fossils in the Luoping Biota

There is decoupling between the preservation of trace fossils and body fossils at Luoping. In particular, the lower and upper fossiliferous units preserve abundant vertebrate and invertebrate fossils, but with only a few superficial trace fossils, such as *Dikoposichnus*, *Megagrapton*, and *Undichna*. Such a decoupling effect has long been recognized by ichnologists, who explain this phenomenon by differential preservational conditions between trace fossils and body fossils (e.g. Buatois and Mángano, 2011a). Indeed, at Luoping, such decoupling might have resulted from periodic anoxia in offshore environments, which largely inhibited colonization by trace makers. The upper and lower fossiliferous units are both characterized by thin-bedded marly carbonate mudstones intercalated with shales, representing quiet, offshore depositional environments. The black sediments, and the common occurrence of dispersed pyrite crystals suggests possible periodic anoxia in offshore environments. Statistical analysis of the pyrite framboids in carbonate mudstones supports such a notion. Measurements of pyrite framboids from two strata of the lower fossiliferous bed/unit of the SSK section reveal mean diameters of 6.60 μm and 5.34 μm, with standard deviations of 1.21 and 1.77, respectively (Fig. 8A–D). This result indicates an anoxic marine environment (e.g. Wilkin et al., 1996; Wignall and Newton, 1998).

Due to such periodic anoxia in bottom waters, bioturbation was largely inhibited. When there were transient oxic conditions, fishes, marine reptiles, and a few invertebrates could survive and leave their traces of activity, represented by the occurrence of *Undichna*, *Dikoposichnus*, and *Megagrapton*. It is noted that the presence of *Undichna* and *Dikoposichnus*, together with the abundant preservation of fishes and marine reptile fossils in the Middle Triassic Luoping biota may reflect the déjà vu effect (*sensu* Buatois and Mángano, 2011b).

Interestingly, at Luoping, the preservational conditions of the Luoping Biota seem to have aided the preservation of trace fossils in the lower and upper fossiliferous units. Specifically, the sealing effect of microbial mats played a significant role in the preservation

of both (including coprolites). When the Luoping animals died and settled on the sea floor, the episodic anoxic environment inhibited rapid decay of the animals. With a further sealing effect from microbial mats, animal carcasses were rapidly coated by mats and protected from disarticulation by turbulent currents (e.g. Luo et al., 2013). Such establishment of firmground substrates might have further stabilized the burrowed sediment surfaces, and enhanced the preservation of those surficial traces (e.g. Buatois and Mángano, 2013).

5.2. Comparison with Early Triassic trace fossil assemblages

A four-stage recovery model based on multiple ichnological parameters has been proposed to summarize the recovery process of trace makers at various stages of the Early Triassic (e.g. Twitchett, 2006), which was later adopted by several researchers (e.g. Chen et al., 2011; Hofmann et al., 2011; Luo et al., 2016). Low ichnodiversity, ichnofabric indices, shallow tiering level and small burrow sizes characterize the early recovery stages (e.g. one to two). This is the case for most ichnoassemblages from shallow marine environments dating from Griesbachian to Dienerian (e.g. Chen et al., 2011; Zhao and Tong, 2010; Zhao et al., 2015). Ichnological parameters show substantial increases in Smithian to Spathian strata from certain regions of South China, eastern Australia, and Western United States, where the recovery stage increased to three or four (e.g. Chen et al., 2011; 2012; Mata and Bottjer, 2011; Luo et al., 2016; Feng et al., 2017). However, not all trace makers had recovered to such an advanced stage in the Smithian and Spathian, suggesting marked variation in recovery rate, most likely controlled by the heterogeneous development of oxic facies (Luo et al., 2016).

At Luoping, nine ichnogenera were discovered from the subtidal deposits of Unit A. Key ichnogenera, such as *Rhizocorallium* and *Thalassinoides* are also commonly found. These observations, together with a moderate to high bioturbation level suggest recovery stage four. Burrow sizes of several ichnogenera (e.g. *Planolites*, *Rhizocorallium* and *Thalassinoides*) also show a marked increase compared with their Lower Triassic counterparts. For example, *Planolites* from subtidal environments at Luoping records a mean diameter of 10.5 mm, which is equivalent to that from the Upper Permian Bellerophon Formation of Northern Italy, obviously larger than Lower Triassic *Planolites* from various regions (e.g. Twitchett, 1999; Pruss and Bottjer, 2004; Zonneveld et al., 2010; Chen et al., 2011; 2012; Luo et al., 2016; Feng et al., 2017a; Fig. 9A), except the late Spathian *Planolites* from the Yashan section of South China (Chen et al., 2011). *Rhizocorallium*is rare in the Lower Triassic, with only a few studies mentioning their burrow sizes. The Induan *Rhizocorallium* from the Montney

Formation of Canada has larger burrow widths even compared to late Early Triassic examples (e.g. Zonneveld et al., 2010; Fig. 9B). This might relate to the presence of refugia in those areas, which facilitate the survival of trace makers. Burrow widths of *Rhizocorallium* from the Smithian Sinbad Limestone, and the Spathian Virgin Limestone of the United States are generally less than 26 mm, with average values of 6 mm and 14 mm respectively (Pruss and Bottjer, 2004; Fraiser and Bottjer, 2009). An obvious increase in *Rhizocorallium* burrow size in the Spathian is also revealed by their occurrence in the Spathian Nanlinghu Formation of the Susong section, South China, and in the Tvilligodden Formation of western Spitsbergen (Worsley and Mørk, 2001; Luo, 2014; Luo et al., 2016). Middle Triassic *Rhizocorallium* from Luoping and other regions of the world (e.g. northwestern British Columbia) have comparable size ranges to their Spathian counterparts (e.g. Zonneveld et al., 2010; Fig. 9B). Burrow sizes of *Thalassinoides* also show obvious increases. Lower Triassic occurrences of *Thalassinoides* from Griesbachian strata of Northern Italy, Western Canada, Smithian strata at Susong in South China, and Spathian strata at Yashan (China) and the Western United States have burrow diameters less than 25 mm (e.g. Zonneveld et al., 2010; Hofmann et al., 2011; Pruss and Bottjer, 2004; Chen et al., 2011; Luo, 2014). The average values for these localities are less than 12 mm (Fig. 9C). At Luoping, the maximum burrow diameter of *Thalassinoides* reaches 30 mm, with the average diameter increasing to 17.9 mm. These values are similar to, or even greater than their Middle to Late Permian counterparts (Whidden, 1990; Zhao and Tong, 2010; Lima and Netto, 2012), and Middle Triassic *Thalassinoides* from north-eastern British Columbia (e.g. Zonneveld et al., 2010; Fig. 9C). In summary, the moderate to high ichnodiversity (nine ichnogenera) in the subtidal environments at Luoping, together with moderate to high bioturation indices, the appearance of key ichnotaxa and increases in burrow sizes, represent a recovery stage four, which suggests a more or less fully recovered ichnossemblage in the early Middle Triassic, 7 Myr after the PTME.

It is worth noting that the bioturbation levels in the turbidite deposits in offshore settings are much higher than their surrounding non-turbiditic strata. In addition, various traces, such as *Diplocraterion*, *Planolites*, *Rhizocorallium*, *Sinusichnus*, *Taenidium*, and *Thalassinoides* were found in those beds. Certain traces, such as *Taenidium*, have penetrated sediments to a depth of 5 cm. Such moderate ichnoassemblages and moderate to high bioturbation levels in turbidite beds are interpreted to be the result of the short colonization of transported infaunal animals from proximal settings (*cf.* Grimm and Föllmi, 1994). The low ichnodiversity and low bioturbation level in non-turbiditic strata of offshore environments at Luoping are most likely

674 due to shallow marine anoxia, and this prevents further comparisons and discussion of their
675 implications for recovery of trace makers in such distal shallow marine settings.
676 The offshore transition of Unit C in the Luoping sections is associated with low
677 ichnodiversity and moderate bioturbation indices (BI), which is in contrast to the habitable
678 zone model stating that the lower shoreface to offshore transition zone are ideal for
679 colonization (*cf.* Beatty et al., 2008). The low ichnodiversity and moderate BI in the offshore
680 transition at Luoping could partly relate to the topography of the basin and also its proximity
681 to anoxic offshore settings. Several intraplatform basins were formed during the early Middle
682 to Late Triassic at Luoping and its border areas, where well-preserved faunas were discovered
683 (e.g. Hu et al, 2011; Benton et al., 2013). The restricted circulation and density stratification
684 of the water column in these basins means they are not large in scale, and the shelf region in
685 these basins could be narrow and steep. Such bathymetric topography prevented the
686 development of a habitable zone and long-term colonization (*cf.* Zonneveld et al., 2010). In
687 addition, the proximity of the offshore transition to the anoxic offshore setting at Luoping
688 might also have hampered the bioturbating activities of trace makers in this environmental
689 setting through possible upwelling of deeper anoxic waters.
690
691 *5.3. Implications for ichnofaunal recovery during the Early Triassic*
692
693 Investigations at Luoping support the utility of trace fossils to study the timing of biotic
694 recovery and the processes of trace makers. The subtidal ichnoassemblage is characterized by
695 medium to high ichnodiversity, medium to high bioturbation indices, and a marked increase in
696 burrow size of many traces. These parameters, together with the common appearance of key
697 ichnogenera (e.g. *Rhizocorallium* and *Thalassinoides*), suggests a recovery stage 4 (*sensu*
698 Twitchett, 2006; Pietsch and Bottjer, 2014), thus indicating a full recovery of trace makers in
699 subtidal environments. Ichnological records from adjacent regions also support an obvious
700 recovery of trace makers (Feng et al., 2017c). In contrast, ichnological parameters from
701 regional ichnoassemblages of Lower Triassic successions typically suggest a recovery stage
702 of one and two, with a few data suggesting some recovery until the latest Smithian and
703 Spathian (Twitchett, 1999; Chen et al., 2011; Zhao et al., 2015; Luo et al., 2016; Feng et al.,
704 2017a). However, the ichnological parameters from offshore environments at Luoping show
705 no signs of recovery. This is most likely due to the periodic anoxic bottom water conditions,
706 which would have substantially inhibited the colonization of infaunal animals, but otherwise
707 aided the fine preservation of the Luoping Biota.

After the PTME, marine ecosystems and ecological structures were re-shaped, with the Modern Evolutionary Fauna expanding to dominate in marine settings (Sepkoski et al., 1981; Erwin, 2006; Peters, 2008). The fossil composition of the Luoping Biota highlights this major change, with fishes, marine reptiles and decapod crustaceans comprising the majority of the fossil collections (e.g. Hu et al., 2011; Wen et al., 2012, 2013; Feldmann et al., 2012, 2015; Huang et al., 2013; Schweitzer et al., 2014). Luoping has revealed many new genera and species of arthropods, which suggest a radiation event during the early Middle Triassic (e.g. Feldmann et al., 2012, 2015, 2017; Huang et al., 2013; Schweitzer et al., 2014). Such a change in ecosystem structure was mirrored by the common occurrence of burrow systems (e.g. *Sinusichnus, Rhizocorallium, Spongeliomorpha,* and *Thalassinoides*) made by decapod crustaceans at Luoping. This highlights how the trace fossil assemblages of the early Middle Triassic document the major faunal changes occurring at this time in comparison with Lower Triassic ichnological records.

6. Conclusions

Well-preserved vertebrates and invertebrates from the Luoping Biota of Yunnan Province in South China suggest a stable, fully recovered shallow marine ecosystem in the early Middle Triassic (Anisian). Equally, well-preserved trace fossils found in association with the Luoping Biota provide a template to compare the behaviours and ecological strategies of trace-making organisms from such a recovered ecosystem with those in the delayed recovery interval of the Early Triassic. Trace fossil assemblages from the Luoping Biota have high ichnodiversity, with 14 ichnogenera discovered in the shallow marine environment of an intra-carbonate platform basin. Nine ichnogenera occurred in the subtidal environment. Such medium to high ichnodiversity, together with a marked increase in burrow size and the common occurrence of key ichnotaxa (e.g. *Rhizocorallium* and *Thalassinoides*) suggest a recovery stage of four. In contrast, non-turbiditic strata of the offshore setting record only three ichnogenera, with bioturbation indices never exceeding one. Periodic anoxic bottom water conditions are identified as the main control on such a protracted trace fossil record, which otherwise aided the fine preservation of body fossils of the Luoping Biota. Furthermore, event sedimentation (turbidites) in offshore settings host a medium ichnodiversity and medium bioturbation indices, both interpreted to result from short term

colonization by transported infaunal animals from proximal settings. The occurrence of variable crustacean-made traces (e.g. *Sinusichnus*, *Spongeliomorpha*, and *Thalassinoides*) at Luoping, together with possible evidence of the decapod radiation from body fossils, highlights the value of using trace fossils to document ecosystem restructuring after the PTME.

Acknowledgments

This study was partly supported by the ACRDP discovery grant to G. R. Shi (DP150100690). This research is also supported by two NSFC grants (41572091 and 41772007 to ZQC), two research grants (GBL21410, GPMR201601 to ML) from the State Key Laboratory of Biogeology and Environmental Geology, and State Key Laboratory of Geological Process and Mineral Resources, China University of Geosciences (Wuhan), and China Geological Survey project (DD20160020, 1212011140051, 12120114030601, and 1212010610211). This paper is a contribution to the IGCP 630 "Permian-Triassic climatic and environmental extremes and biotic response".

References

Abbassi, N., 2007. Shallow marine trace fossils from Upper Devonian sediments of the Kuh-E Zard, Zefreh area, central Iran. Iranian Journal of Science & Technology, Transaction A, 31, 23–33.

Allison, P.A., Briggs, D.E.G., 1991. Taphonomy of non-mineralized tissues. In: Allison, P.A., Briggs, D.E.G. (Eds.), Taphonomy: Releasing the Data Locked in the Fossil Record. Plenum Press, New York, 25–69.

Anderson, A., 1976. Fish trails from the Early Permian of South Africa. Palaeontology 19, 397–409.

Bai, J.K., Yin, F.G., Zhang, Q.Y., 2011. Microfacies and enrichment pattern of fossils in the fossiliferous beds of Luoping Biota, Yunnan Province. Geology in China, 38, 393–402 (in Chinese with English abstract).

Baucon, A., Carvalho, C.N.D., 2016. Stars of the aftermath: *Asteriacites* beds from the Lower Triassic of the Carnic Alps (Werfen Formation, Sauris Di Sopra), Italy. Palaios 31, 161–176.

776 Beatty, T.W., Zonneveld, J.P., Henderson, C.M., 2008. Anomalously diverse Early Triassic
777 ichnofossil assemblages in northwest Pangea: a case for shallow-marine habitable zone.
778 Geology 36, 771–774.
779 Belaústegui, Z., de Gibert, J.M., Lopez-Blanco, M., Bajo, I., 2014. Recurrent constructional
780 pattern of the crustacean burrow *Sinusichnus sinuosus* from the Paleogene and Neogene
781 of Spain. Acta Palaenotol. Pol. 59, 461–474.
782 Benner, J.S., Ridge, J.C., Knecht, R.J., 2009. Timing of post-glacial reinhabitation and
783 ecological development of two New England, USA, drainages based on trace fossil
784 evidence. Palaeogeogr. Palaeoclimatol. Palaeoecol. 272, 212–231.
785 Benton, M.J., Zhang, Q.Y., Hu, S.X., Chen, Z.Q., Wen, W., Liu, J., Huang, J.Y., Zhou, C.Y.,
786 Xie, T., Tong, J.N., Choo, B., 2013. Exceptional vertebrate biotas from the Triassic of
787 China, and the expansion of marine ecosystems after the Permo-Triassic mass extinction.
788 Earth-Sci. Rev. 125, 199–243.
789 Bradshaw, M.A., 1981. Palaeoenvironmental interpretations and systematics of Devonian
790 trace fossils from the Taylor Group (Lower Beacon Supergroup), Antarctica. New
791 Zealand J. Geol. Geophysics, 24, 615–652.
792 Bradshaw, M.A., 2010. Devonian trace fossils of the Horlick Formation, Ohio Range,
793 Antarctica: systematic description and palaeoenvironmental interpretation. Ichnos 17, 58–
794 114.
795 Bromley, R.G., 1996. Trace Fossils. Biology, Taphonomy and Applications. London:
796 Chapman & Hall. 361 pp.
797 Bromley, R.G., Asgaard, U., 1979. Triassic freshwater ichnocoenoses from Carlsberg Fjord,
798 East Greenland. Palaeogeogr. Palaeoclimatol. Palaeoecol. 28, 39–80.
799 Bromley, R.G., Frey, R.W., 1974. Redescription of the trace fossil *Gyrolithes* and taxonomic
800 evaluation of *Thalassinoides, Ophiomorpha* and *Spongeliomorpha*. Bull. Geol. Soc.
801 Denmark 23, 311–335.
802 Buatois, L.A., Mángano, M.G., 2002. Trace fossils from Carboniferous floodplain deposits in
803 western Argentina: implications for ichnofacies models of continental environments.
804 Palaeogeogr. Palaeoclimatol. Palaeoecol 183, 71–86.
805 Buatois, L.A., Mángano, M.G., 2011a. Ichnology: Organism-Substrate Interaction in Space
806 and Time. Cambridge University Press, New York, 358 pp.
807 Buatois, L.A., Mángano, M.G., 2011b. The déjà vu effect: recurrent patterns in exploitation of
808 ecospace, establishment of the mixed layer, and distribution of matgrounds. Geology 39,
809 1163–1166.

Buatois, L.A., Mángano, M.G., 2013. Ichnodiversity and ichnodisparity: significance and caveats. Lethaia 46, 281–292.

Buatois, L.A., Macsotay, O., Quiroz, L.I., 2009. *Sinusichnus*, a trace fossil from Antartica and Venezuela: expanding the datasets of crustacean burrows. Lethaia 42, 511–518.

Buckman, J.O., 1994. *Archaeonassa* Fenton and Fenton 1937 reviewed. Ichnos 3, 185–192.

Bustillo, M.A., Ruiz-Ortiz, P.A., 1987. Chert occurrence in carbonate turbidites: example from the Upper Jurassic of the Betic Mountains (southern Spain). Sedimentology 34, 611–621.

Carmona, N.B., Buatois, L.A., Mángano, M.G., 2004. The trace fossil record of burrowing decapod crustaceans: evaluating evolutionary radiations and behavioural convergence. Fossil and Strata 51, 141–153.

Carvalho, C.N.D., Viegas, P.A., Cachão, M., 2007. *Thalassinoides* and its producer: populations of *Mecochirus* buried within their burrow system, Boca Do Chapim Formation (Lower Cretaceous), Portugal. Palaios 22, 104–109.

Chen, Z.Q., Benton, M.J., 2012. The timing and pattern of biotic recovery following the end-Permian mass extinction. Nat. Geosci. 5, 375–383.

Chen, Z.Q., Fraiser, M.L., Bolton, C., 2012. Early Triassic trace fossils from Gondwana Interior Sea: Implication for ecosystem recovery following the end-Permian mass extinction in south high-latitude region. Gondwana Res. 22, 238–255.

Chen, Z.Q., Tong, J.N., Fraiser, M.L., 2011. Trace fossil evidence for restoration of marine ecosystems following the end-Permian mass extinction in the Lower Yangtze region, South China. Palaeogeogr. Palaeoclimatol. Palaeoecol. 299, 449–474.

Chen, Z.Q., Yang, H., Luo, M., Benton, M.J., Kaiho, K., Zhao, L.S., Huang, Y.G., Zhang, K.X., Fang, Y.H., Jiang, H.S., Qiu, H., Li, Y., Tu, C.Y., Shi, L., Zhang, L., Feng, X.Q., Chen, L., 2015. Complete biotic and sedimentary records of the Permian-Triassic transition from Meishan section, South China: ecologically assessing mass extinction and its aftermath. Earth Sci. Rev. 149, 67–107.

D'Alessandro, A., Bromley, R.G., 1987. Meniscate trace fossils and the *Muensteria-Taenidium* problem. Palaeontology 30, 743–763.

Ding, Y., Cao, C.Q., Zheng, Q.F., 2016. Lopingian (Upper Permian) trace fossils from the northern Penglaitan Section, Laibin, Guangxi, South China and their environmental implications. Palaeoworld 25, 377–387.

Dott, R.H., Bourgeois, J., 1982. Hummocky stratification: significance of its variable bedding sequences. Geol. Soc. Am. Bull. 93, 663–680.

844 Dumas, S., Arnott, R.W.C. 2006. Origin of hummocky and swaley cross-stratification–the
845 control influence of unidirectional current strength and aggradation rate. Geology 34,
846 1073–1075.
847 Enos, P., Lehrmann, D.J., Wei, J.Y., Yu, Y.Y., Xiao, J.F., Chaikin, D.H., Minzoni, M., Berry,
848 A.K., Montgomery, P., 2006. Triassic Evolution of the Yangtze Platform in Guizhou
849 Province, People's Republic of China. Geol. Soc. Am. Special Papers 417, 1–105.
850 Erwin, D.H., Bowring, S.A., Jin, Y.G., 2002. End-Permian mass extinction: a review. In:
851 Koeberl, C., MacLeod, K.G. (Eds.), Catastrophic events and Mass Extinctions: Impacts
852 and Beyond. Geol. Soc. Am. Special Paper 256, pp. 353–383.
853 Erwin, D.H., 2006. Extinction: How Life on Earth Nearly Ended 250 Million Years Ago.
854 Princeton University Press, Princeton, 296 pp.
855 Ezaki, Y., Liu, J.B., Nagano, T., Adachi, N., 2008. Geobiological aspects of the earliest
856 Triassic microbialites along the southern periphery of the tropical Yangtze Platform:
857 initiation and cessation of a microbial regime. Palaios 23, 356–369.
858 Ezaki, Y., Liu, J.B., Adachi, N., 2012. Lower Triassic stromatolites in Luodian County,
859 Guizhou Province, South China: evidence for the protracted devastation of the marine
860 environments. Geobiology 10, 48–59.
861 Feldmann, R.M., Schweitzer, C.E., Hu, S.X., Zhang, Q.Y., Zhou, C.Y., Xie, T., Huang, J.Y.,
862 Wen, W., 2012. Macrurous Decapoda from the Luoping biota (Middle Triassic) of China.
863 J. Paleontol. 86, 425–441.
864 Feldmann, R.M., Schweitzer, C.E., Hu, S.X., Huang, J.Y., Zhou, C.Y., Zhang, Q.Y., Wen,
865 W., Xie, T., Maguire, E., 2015. Spatial distribution of Crustacea and associated organisms
866 in the Luoping biota (Anisian, Middle Triassic), Yunnan Province, China: evidence of
867 periodic mass kills. J. Paleontol. 89, 1022–1037.
868 Feng, X.Q., Chen, Z.Q., Woods, A., Fang, Y.H., 2017a. A Smithian (Early Triassic)
869 ichnoassemblage from Lichuan, Hubei Province, South China: implications for biotic
870 recovery after the latest Permian mass extinction. Palaeogeogr. Palaeoclimatol.
871 Palaeoecol. 486, 123–141.
872 Feng, X.Q., Chen, Z.Q., Bottjer, D.J., Fraiser, M.L., Xu, Y.L., Luo, M., 2017b. Additional
873 records of ichnogenus *Rhizocorallium* from the Lower and Middle Triassic, south China:
874 implications for biotic recovery after the end-Permian mass extinction. GSA Bull. (in
875 press).
876 Feng, X.Q., Chen, Z.Q., Woods, A., Wu, S.Q., Fang, Y.H., Luo, M., Xu, Y.L., 2017c. Anisian
877 (Middle Triassic) marine ichnocoenoses from the eastern and western margins of the

878 Kamdian Continent, Yunnan Province, SW China: implications for the Triassic biotic
879 recovery. Glob. Planet. Chang. 157, 194–213.
880 Feng, Z.Z., Bao, Z.D., Li, S.W., 1997. Lithofacies paleogeography of Middle and Lower
881 Triassic of South China. Petroleum Industry Press, Beijing, pp. 1–222 (in Chinese with
882 English abstract).
883 Fenton, C.L., Fenton, M.A., 1937. *Archaeonassa*, Cambrian snail trails and burrows.
884 American Midland Naturalist 18, 454–456.
885 Fillmore, D.L., Lucas, S.G., Simpson, E.L., 2011. The fish swimming trace *Undichna* from
886 the Mississippian Mauch Chunk Formation, Eastern Pennsylvania. Ichnos 18, 27–34.
887 Flügel, E., 2004. Microfacies of carbonate rocks: analysis, interpretation and application.
888 Springer, New York, pp. 1–976.
889 Foster, W.J., Twitchett, R.J., 2014. Functional diversity of marine ecosystems after the Late
890 Permian mass extinction event. Nat. Geosci. 7, 233–238
891 Fraiser, M.L., Bottjer, D.J., 2009. Opportunistic behavior of invertebrate marine tracemakers
892 during the Early Triassic aftermath of the end-Permian mass extinction. Aust. J. Earth
893 Sci. 56, 841–857.
894 Gibert, J.M.de., 2001. *Undichna gosiutensis*, isp. nov.: a new fish trace fossil from the
895 Jurassic of Utah. Ichnos 8, 15–22.
896 Gibert, J.M.de., Martinell, J., 1996. Trace fossil assemblages and their palaeoenvironmental
897 significance in the Pliocene marginal marine deposits of the Baix Ebre (Catalonia, NE
898 Spain). Géologie Méditerranéenne 23, 211–225.
899 Gibert, J.M.de., 1996. A new decapod burrow system from the NW Mediterranean Pliocene.
900 Revista Española de Paleontología 11, 251–254.
901 Gibert, J.M.de., Jeong, K., Martinell, J. 1999a. Ethologic and ontogenic significance of the
902 Pliocene trace fossil *Sinusichnus sinuosus* from the northwestern Mediterranean. Lethaia
903 32, 31–40.
904 Gibert, J.M.de., Buatois, L.A., Fregenal-Martinez, M.A., Mangano, M.G., Ortega, F., Poyato-
905 Ariza, F.J., Wenz, S., 1999b. The fish trace fossil *Undichna* from the Cretaceous of
906 Spain. Palaeontology 42, 409–427.
907 Godbold, A., Schoepfer, S., Shen, S.Z., Henderson, C.M., 2017. Precarious ephemeral
908 refugia during the earliest Triassic. Geology 45, 607–610.
909 Graham, J.R., Pollard, J.E., 1982. Occurrence of the trace fossil Beaconites antarcticus in the
910 lower Carboniferous fluviatile rocks of county Mayo, Ireland. Palaeogeogr.
911 Palaeoclimatol. Palaeoecol. 38, 257–268.

912 Grimm, K.A., Follmi, K.B., 1994. Doomed pioneers: allochthonous crustacean tracemakers in
913 anaerobic basinal strata, Oligo-Miocene San Gregorio Formation, Baja California Sur,
914 Mexico. Palaios 9, 313–334.
915 Hall, J., 1847. Paleontology of New York. Volumn 1, C. Van Benthuysen, Albany, 362 pp.
916 Häntzschel, W., 1975. Trace fossil and Problematica. In: Teichert, C. (ed.), Treatise on
917 Invertebrate Paleontology, Part W, Miscellanea, Supplement I, Geological Society of
918 America and University of Kansas Press, pp. 1–269.
919 Heer, O., 1877. Flora Fossilis Helvetiae. Vorweltliche Flora der Schweiz. J. Wurster &
920 Comp., Zurich, 182 pp.
921 Hofmann, R., Goudemand, N., Wasmer, M., Bucher, H., Hautmann, M., 2011. New trace
922 fossil evidence for an early recovery signal in the aftermath of the end–Permian mass
923 extinction. Palaeogeogr. Palaeoclimatol. Palaeoecol. 310, 216–226.
924 Hofmann, R., Buatois, L.A., MacNaughton, R.B., Mangano, M.G., 2015. Loss of sedimentary
925 mixed layer as a result of the end-Permian extinction. Palaeogeogr. Palaeoclimatol.
926 Palaeoecol. 428, 1–11.
927 Hu, S.L., Li, Y.J., Dai, M., Pu, Z.P., 1996. The laser mass-spectrometer ^{40}Ar–^{49}Ar age of
928 green pisolites of Guizhou Province. Acta Petrol. Sin. 12, 409–415 (in Chinese).
929 Hu, S.X., Zhang, Q.Y., Chen, Z.Q., Zhou, C.Y., Lv, T., Xie, T., Wen, W., Huang, J.Y.,
930 Benton, M.J., 2011. The Luoping biota: exceptional preservation, and new evidence on
931 the Triassic recovery from end-Permian mass extinction. Proc. R. Soc. B 278, 2274–
932 2283.
933 Huang, J.Y., Feldmann, R.M., Schweitzer, C.E., Hu, S.X., Zhou, C.Y., Benton, M.J., Zhang,
934 Q.Y., Wen, W., Xie, T., 2013. A new shrimp (Decapoda, Dendrobranchiata, Penaeoidea)
935 from the Middle Triassic of Yunnan, Southwest China. J. Paleont. 87, 603–611.
936 Huang, J.Y., Zhang, K.X., Zhang, Q.Y., Lv, T., Zhou, C.Y., Bai, J.K., 2009. Conodonts
937 stratigraphy and sedimentary environment of the Middle Triassic at Daaozi Section of
938 Luoping county, Yunnan province, South China. Acta Micropalaeontologica Sinica 26,
939 211–224 (In Chinese with English abstract).
940 Hull, P., Darroch, S.A.F., 2013. Mass extinction and the structure and function of ecosystem.
941 In: Bush, A., Pruss, S.B., Payne, J.L. (Eds.), Ecosystem Paleobiology and Geobiology,
942 The Paleontological Society Papers 19, 1–42.
943 Jame, N.P., Bourque, P.A., 1992. Reefs and Mounds. In: Walker, R.G., James, N.P (Eds.),
944 Facies Models: response to sea level change. Geological Association of Canada, St.
945 John's, pp. 323–348.

946 Keighley, D.G., Pickerill, R.K., 1994. The ichnogenus *Beaconites* and its distinction from
947 *Ancorichnus* and *Taenidium*. Palaeontology 37, 305–337.
948 Knaust, D., 2007. Invertebrate trace fossils and ichnodiversity in shallow-marine carbonates
949 of the German Middle Triassic (Muschelkalk). In: Bromley, R.G., Buatois, L.A.,
950 Mangano, G., Genise, J.F., Melchor, R.N., (Eds.), Sediment-Organism Interactions: a
951 multifaceted ichnology. SEPM Special Publication 88, pp. 223–240.
952 Knaust, D., 2010. The end-Permian mass extinction and its aftermath on an equatorial
953 carbonate platform: insights from ichnology. Terra Nova 22, 195–202.
954 Knaust, D., 2013. The ichnogenus *Rhizocorallium*: classification, trace makers,
955 palaeoenvironments and evolution. Earth Sci. Rev. 126, 1–47.
956 Knaust, D., Uchman, A., Hagdorn, H., 2016. The probable isopod burrow *Sinusichnus*
957 *seilacheri* isp. n. from the Middle Triassic of Germany: an example of behavioural
958 convergence. Ichnos 24, 138–146.
959 Kotake, N., 1992. Deep-sea echiurans: possible producers of *Zoophycos*. Lethaia 25, 311–316.
960 Książkiewicz, M., 1968. O niektórych problematykach z fliszKarpat polskich, Część III.
961 Rocznik Polskiego Towarzystwa Geologicznego 38, 3–17.
962 Książkiewicz, M., 1977. Trace fossils in the flysch of the Polish Carpathians. Palaeontol. Pol.
963 36, 1–208.
964 Lehrmann, D.J., Enos, P., Payne, J.L., Montgomery, P., Wei, J.Y., Yu, Y.Y., Xiao, J.F.,
965 Orchard, M.J., 2005. Permian and Triassic depositional history of the Yangtze platform
966 and Great Bank of Guizhou in the Nanpanjiang Basin of Guizhou and Guangxi, South
967 China. Albertiana 33, 149–168.
968 Lima, J.H., Netto, R.G., 2012. Trace fossils from the Permian Teresina Formation at Cerro
969 Caveiras (S Brazil). Revista Brasileira de Paleontology 15, 5–22.
970 Liu, J., Hu, S.X., Rieppel, O., Jiang, D.Y., Benton, M.J., Kelley, N.P., Aitchison, J.C., Zhou,
971 C.Y., Wen, W., Huang, J.Y., Xie, T., Lv, T., 2014. A gigantic nothosaur (Reptilia:
972 Sauropterygia) from the Middle Triassic of SW China and its implication for the Triassic
973 biotic recovery. Sci. Rep. 4, e7142.
974 Luo, M., 2014. Early Triassic trace fossils from South China: implications for biotic recovery
975 from the end-Permian Mass Extinction. The University of Western Australia.
976 Unpublished PhD thesis. 1–222.
977 Luo, M., Chen, Z.Q., 2014. New arthropod traces from the Lower Triassic Kockatea Shale
978 Formation, northern Perth Basin, Western Australia: ichnology, taphonomy and
979 palaeoecology. Geological J. 49, 163–176.

980 Luo, M., Chen, Z.Q., Hu, S.X., Zhang, Q.Y., Benton, M.J., Zhou, C.Y., Wen, W., Huang,
981 J.Y., 2013. Carbonate reticulated ridge structures from the lower Middle Triassic of the
982 Luoping area, Yunnan, southwestern China: Geobiologic features and implications for
983 exceptional preservation of the Luoping Biota. Palaios 28, 541–551.
984 Luo, M., George, A.D., Chen, Z.Q., 2016. Sedimentology and ichnology of two Lower
985 Triassic sections in South China: implications for the biotic recovery from the end-
986 Permian Mass extinction. Glob. Planet. Chang. 144, 198–212.
987 Luo, M., Hu, S.X., Benton, M.J., Zhao, L.S., Huang, J.Y., Song, H.J., Wen, W., Zhang, Q.Y.,
988 Fang, Y.H., Huang, Y.G., Chen, Z.Q., 2017. Taphonomy and palaeobiology of early
989 Middle Triassic coprolites from the Luoping biota, southwest China: implications for
990 reconstruction of fossil food webs. Palaeogeogr. Palaeoclimatol. Palaeoecol. 474, 223–
991 246.
992 MacEachern, J.A., Bann, K.L., Gingras, M.K., Zonneveld, J.P., Dashtgard, S.E., Pemberton,
993 S.G., 2012. The ichnofacies paradigm. In: Knaust, D., Bromley, R.G., (Eds.), Trace
994 Fossils as Indicators of Sedimentary Environments. Developments in Sedimentology 64,
995 103–138.
996 MacEachern, J.A., Bann, K.L., Pemberton, S.G., Gingras, M.K., 2007. The ichnofacies
997 paradigm: high resolution paleoenvironmental interpretation of the rock record. In:
998 MacEachern, J.A., Gingras, M.K., Pemberton, S.G. (Eds.), Applied Ichnology. SEPM
999 Short Course Notes 52, 27–46.
1000 Massalongo, A., 1855. *Zoophycos*, novum genus plantorum fossilium. Antonelli, Verona, 52
1001 pp.
1002 Mata, S.C., Bottjer, D.J., 2011. Origin of Lower Triassic microbialites in mixed carbonate–
1003 siliciclastic successions: ichnology, applied stratigraphy, and the end-Permian mass
1004 extinction. Palaeogeogr. Palaeoclimatol. Palaeoecol. 300, 158–178.
1005 McBride, E.F., Folk, R.L., 1979. Features and origin of Italian Jurassic radiolarites deposited
1006 on continental crust. J. Sediment. Petrol. 49, 838–868.
1007 McGhee, G.R., Sheehan, P.M., Bottjer, D.J., Droser, M.L., 2004. Ecological ranking of
1008 Phanerozoic biodiversity crises: ecological and taxonomic severities are decoupled.
1009 Palaeogeogr. Palaeoclimatol. Palaeoecol. 211, 289–297.
1010 Melchor, R.N., Bromley, R.G., Bedatou, E., 2009. *Spongeliomorpha* in nonmarine settings: an
1011 ichnotaxonomic approach. Earth Environment. Sci. Trans. R. Soc. Edinburgh 100, 429–
1012 436.

1013 Morrissley, L.B., Braddy, S.J., S.J., Bennett, J.P., Marriott, S.B., Tarrant, P.R., 2004. First
1014 trails from the Lower Old Red Sandstone of Tredomen Quarry, Powys, southeast Wales.
1015 Geological J. 38, 337–358.
1016 Morrow, J.R., Hasiotis, S.T., 2007. Endobenthic response through mass extinction episodes:
1017 predictive models and observed patterns. In: Miller III, W. (Ed.), Trace Fossils: Concepts,
1018 Problems, Prospects. Elsevier, Amsterdam, pp. 575–598.
1019 Myrow, P.M., 1995. *Thalassinoides* and the enigma of early Paleozoic open-framework
1020 burrow systems. Palaios 10, 58–74.
1021 Nicholson, H.A., 1873. Contributions to the study of the errant annelids of the older
1022 Palaeozoic rock. Proc. R. Soc. London. 21, 288–290.
1023 Olóriz, F., Rodríguez-Tovar, F.J., 2000. *Diplocraterion*: A useful marker for sequence
1024 stratigraphy and correlation in the Kimmeridgian, Jurassic (Prebetic Zone, Betic
1025 Cordillera, southern Spain). Palaios 15, 546–552.
1026 Osgood, R.G., 1970. Trace fossils of the Cincinnati area. Palaeontographica Americana, 6,
1027 277–444.
1028 Pemberton,S.G., Frey, R.W., 1982. Trace fossil nomenclature and the
1029 *Planonites–Palaeophycus* dilemma. J. Paleontol. 56, 843–881.
1030 Peters, S.E., 2008. Environmental determinants of extinction selectivity in the fossil record.
1031 Nature 454, 626–629.
1032 Pietsch, C., Bottjer, D.J., 2014. The importance of oxygen for the disparate recovery patterns
1033 of the benthic macrofauna in the Early Triassic. Earth Sci. Rev. 137, 65–84.
1034 Pruss, S.B., Bottjer, D.J., 2004. Early Triassic trace fossils of the Western United States and
1035 their implications for prolonged environmental stress from the end-Permian Mass
1036 Extinction. Palaios 19, 551–564.
1037 Reineck, H.E., 1963. Sedimentgefüge im Bereich der südliche Nordsee. Abhandlungen
1038 Senckenbergischen Naturforsche de Gesellschaft, 505, 1–138.
1039 Schweitzer, C.E., Feldmann, R.M., Hu, S.X., Huang, J.Y., Zhou, C.Y., Zhang, Q.Y., Wen,
1040 W., Xie, T., 2014. Penaeoid Decapoda (Dendrobranchiata) from the Luoping biota
1041 (Middle Triassic) of China: systematics and taphonomic framework. J. Paleontol. 88,
1042 457–474.
1043 Seilacher, A., 1974. Flysch trace fossils: evolution of behavioural diversity in the deep-sea.
1044 Neues Jahrbuch für Geologie und Paläontologie, Monatshefte 4, 233–245.
1045 Sepkoski, J.J., Bambach, R.K., Raup, D.M., Valentine, J.W., 1981. Phanerozoic marine
1046 diversity and the fossil record. Nature, 293, 435–437.

1047 Shi, G., Woods, A., Yu, M.Y., Wei, H.Y., 2015. Two episodes of evolution of trace fossils
1048 during the Early Triassic in the Guiyang area, Guizhou Province, South China.
1049 Palaeogeogr. Palaeoclimatol. Palaeoecol. 426, 275–284.
1050 Sperling, E.A., 2013. Tackling the 99%: can we begin to understand the paleoecology of the
1051 small and soft-bodied animal majority? In: Bush, A., Pruss, S.B., Payne, J. (Eds.),
1052 Ecosystem Paleobiology and Geobiology. The Paleontological Society Papers 19, 77–86.
1053 Stockar, R., 2010. Facies, depositional environment, and palaeoecology of the Middle Triassic
1054 Cassina beds (Meride Limestone, Monte San Giorgio, Switzerland). Swiss J. Geosci. 103,
1055 101–119.
1056 Taylor, A.M., Gawthorpe, R.L., 1993. Application of sequence stratigraphy and trace fossil
1057 analysis to reservoir description: Examples from the Jurassic of the North Sea. In Parker,
1058 J.R., ed., Petroleum Geology of Northwest Europe: Proceedings of the 4th Conference:
1059 Geological Society, London, 317–335.
1060 Taylor, A.M., Goldring, R., 1993. Description and analysis of bioturbation and ichnofabric. J.
1061 Geol. Soc. 150, 141–148.
1062 Torell, O.M., 1870. Petrificata Suecana Formationis Cambricae. Lunds Universitets Årsskrift,
1063 6, 1–14.
1064 Twitchett, R.J., 1999. Palaeoenvironments and faunal recovery after the end-Permian Mass
1065 Extinction. Palaeogeogr. Palaeoclimatol. Palaeoecol. 154, 27–37.
1066 Twitchett, R.J., 2006. The palaeoclimatology, palaeoecology and palaeoenvironmental
1067 analysis of mass extinction events. Palaeogeogr. Palaeoclimatol. Palaeoecol. 232, 190–
1068 213.
1069 Twitchett, R.J., Barras, C.G., 2004. Trace fossils in the aftermath of mass extinction events.
1070 In: McIlroy, D. (Ed.), Application of Ichnology to Palaeoenvironmental and Stratigraphic
1071 Analysis: Geological Society of London, Special Publication, 228, pp. 395–415.
1072 Twitchett, R.J., Wignall, P.B., 1996. Trace fossils and the aftermath of the Permo–Triassic
1073 mass extinction: evidence from northern Italy. Palaeogeogr. Palaeoclimatol. Palaeoecol.
1074 124, 137–151.
1075 Uchman, A., 1995. Taxonomy and palaeoecology of flysch trace fossils: The Marnoso-
1076 arenacea Formation and associated facies (Miocene, Northern Apennines, Italy).
1077 Beringeria 15, 1–115.
1078 Uchman, A., 1998. Taxonomy and ethology of flysch trace fossils: revision of the marian
1079 Książkiewicz collection and studies of complementary materials. Annales Societatis
1080 Geologorum Poloniae 68, 105–218.

1081 Uchman, A., Hanken, N. M., Nielsen, J. K., Grundvåg, S.A., Piasecki, S., 2016. Depositional
1082 environment, ichnological features and oxygenation of Permian to earliest Triassic marine
1083 sediments in central Spitsbergen, Svalbard. Polar Res. 35, e24782.
1084 Vossler, S.M., Pemberton, S.G., 1988. *Skolithos* in the Upper Cretaceous Cardium Formation:
1085 an ichnofossil example of opportunistic ecology. Lethaia 21, 351–362.
1086 Walker, R.G., 1992. Turbidites and submarine fans. In: Walker, R.G., James, N.P (Eds.),
1087 Facies Models: response to sea level change. Geological Association of Canada, St.
1088 John's, pp. 239–264.
1089 Wen, W., Zhang, Q.Y., Hu, S.X., Zhou, C.Y., Xie, T., Huang, J.Y., Chen, Z.Q., Benton,M.J.,
1090 2012. A new basal actinopterygian fish from the Anisian (Middle Triassic) of Luoping,
1091 Yunnan Province, Southwest China. Acta Palaeontol. Pol. 57, 149–160.
1092 Wen,W., Zhang, Q.Y., Hu, S.X., Benton, M.J., Zhou, C.Y., Xie, T., Huang, J.Y., Chen, Z.Q.,
1093 2013. Coelacanths from the Middle Triassic Luoping biota, Yunnan, South China, with
1094 the earliest evidence of ovoviviparity. Acta Palaeontol. Pol. 58, 175–193.
1095 Whidden, K.J., 1990. Preferential silicification of trace and body fossils in the Fossil
1096 Mountain Member of the Permian Kaibab Formation (southwestern Utah): Unpublished
1097 M.S Thesis, University of Southern California, Los Angeles, 158 pp.
1098 Wignall, P.B., Hallam, A., Lai, X.L., Yang, F.Q., 1995. Palaeoenvironmental changes across
1099 the Permian/Triassic boundary at Shangshi (N. Sichuan, China). Historical Biol. 10, 175–
1100 189.
1101 Wignall, P.B., Morante, R., Newton, R., 1998. The Permo–Triassc transition in Spitsbergen:
1102 δ^{13}Corg chemostratigraphy, Fe and S geochemistry, facies, fauna and trace fossils. Geol.
1103 Mag. 135, 47–62.
1104 Wignall, P.B., Newton, R., 1998. Pyrite framboid diameter as a measure of oxygen deficiency
1105 in ancient mudrocks. Am. J. Sci. 298, 537–552.
1106 Wilkin, R.T., Barnes, H.L., Brantley, S.L., 1996. The size distribution of framboidal pyrite in
1107 modern sediments: an indicator of redox conditions. Geochim. Cosmochim. Acta 60,
1108 3897–3912.
1109 Worsley, D., Mørk, A., 2001. The environmental significance of the trace fossil
1110 *Rhizocorallium jenense* in the Lower Triassic western Spitsbergen. Polar Res. 20, 37–48.
1111 Yochelson, E.L., Fedonkin, M.A., 1997. The type specimens (Middle Cambrian) of the trace
1112 fossil *Archaeonassa* Fenton and Fenton. Can. J. Earth. Sci. 34, 1210–1219.
1113 Zhang, Q.Y., Wen,W., Hu, S.X., Benton, M.J., Zhou, C.Y., Xie, T., Lu, T., Huang, J.Y.,
1114 Choo, B., Chen, Z.Q., Liu, J., Zhang, Q.C., 2014. Nothosaur foraging tracks from the

Middle Triassic of Southwestern China. Nat. Commun. 5, 3973e, DOI: 10.1038/ncomms4973.

Zhang, Q.Y., Zhou, C.Y., Lu, T., Xie, T., Lou, X.Y., Liu, W., Sun, Y.Y., Wang, X.S., 2008a. Discovery and significance of the Middle Triassic Anisian Biota. Geol. Rev. 54, 523–527 (in Chinese with English abstract).

Zhang, Q.Y., Zhou, C.Y., Lu, T., Xie, T., Lou, X.Y., Liu, W., Sun, Y.Y., Huang, J.Y., Zhao, L.S., 2009. A conodont-based Middle Triassic age assignment for the Luoping Biota of Yunnan, China. Science in China Series D: Earth Sciences 52, 1673−1678.

Zhang, L.J., Fan, R.Y., Gong, Y.M., 2015. *Zoophycos* macroevolution since 541 Ma. Sci. Rep. 4, e14954.

Zhang, X.H., Shi, G.R., Gong, Y.M., 2008b. Middle Jurassic trace fossils from the Ridang Formation in Sajia County, South Tibet, and their palaeoenvironmental significance. Facies 54, 45–60.

Zhao, X.M., Tong, J.N., 2010. Two episodic changes of trace fossils through the Permian-Triassic transition in the Meishan cores, Zhejiang Province. Sci. China Ser. D Earth Sci. 53, 1885–1893.

Zhao, X.M., Tong, J.N., Yao, H.Z., Niu, Z.J., Luo, M., Huang, Y.F., Song, H.J., 2015. Early Triassic trace fossils from the Three Gorges area of South China: implications for the recovery of benthic ecosystems following the Permian-Triassic extinction. Palaeogeogr. Palaeoclimatol. Palaeoecol. 429, 100–116.

Zenker, J.C., 1836. Historisch-topographisches Taschenbuch von Jena und seiner Umgebung. Friedrich Frommann, Jena. 1–338.

Zonneveld, J.P., 2011. Suspending the rules: unravelling the ichnological significance of the Lower Triassic post-extinction recovery interval. Palaios 26, 677–681.

Zonneveld, J.P., Gingras, M.K., Pemberton, S.G., 2001. Trace fossil assemblages in a Middle Triassic mixed siliciclastic–carbonate marginal marine coastal depositional system, British Columbia. Palaeogeogr. Palaeoclimatol. Palaeoecol. 166, 249–276.

Zonneveld, J.P., Gingras, M.K., Beatty, T.W., 2010. Diverse ichnofossil assemblage following the P-T mass extinction, Lower Triassic, Alberta and British Columbia, Canada: evidence for shallow marine refugia on the northwestern coast of Pangaea. Palaios 25, 368–392.

Figure and Figure captions

Fig. 1.A, Location of the three studied sections (stars) at Luoping, Yunnan Province of South China. Note the insert map (B) only shows mainland China. B, Middle Triassic palaeogeographic map of South China showing the palaeogeographic setting of Luoping and adjacent areas [base map modified from Feng et al., (1997)].

Fig. 2. Stratigraphic columns showing the distribution of trace fossils and bioturbation levels of the three studied representative sections at Luoping, Yunnan Province. The bioturbation scheme follows Reineck (1963) and Taylor and Goldring (1993). Abundant invertebrate and vertebrate fossils occur in the Dawazi, Xiangdongpo, and Shangshikan sections, which are abbreviated as DWZ, XDP, and SSK, respectively. Note, the nodular, bioturbated carbonate wackestone is here applied as a marker bed to correlate the trace fossil records of the three sections.

Fig. 3. Field photos showing the typical rock types and sedimentary structures within each unit of the three sections. A, oncoidal packstone-wackestone, bed 2, XDP. Note the individual oval to irregular shaped oncoids (arrowed); B, laminated marly carbonate mudstone, bed 26–27, SSK. Note the very thin-bedded chert layers (arrowed) intercalated in marly carbonate mudstone. Hammer is 39 cm long; C, plan view of carbonate reticulated ridge structures. Bed 88, XDP; D, Turbidite deposits from the XDP section, bed 55. The sharp-based, normally graded wacke-packestone layer is overlain by very thin layers of planar- to convolute-laminated carbonate mudstone and structureless carbonate mudstone. They are here interpreted to represent Ta, Tb+Tc and Te of the Bouma turbiditic sequence. E, nodular carbonate wackestone and overlying marly carbonate mudstone. XDP, bed 73 and 74. F, Hummocky cross-stratified carbonate wackestone; XDP, bed 136. G, thick-bedded carbonate mudstone, with planar lamination. XDP, bed 167 and 168. H, laminated stromatolitic dolomite, bed 187, DWZ.

Fig.4. Field photos showing trace fossils from the Middle Triassic Guanling Formation. A, Horizontal *Archaeonassa* (arrowed); bed 9, SSK; B, *Arenicolites*; bed 2, XDP; C, *Dikoposichnus*; bed 34, SSK; Note the two black arrows indicating the single imprints made by animal limbs. White arrow indicates direction of movement of the trace maker. D–E, Enlargement of *Diplocraterion* isp. from bed 42, SSK. Note the paired tube with spreiten,

characterizing *Diplocraterion*. F, Dense *Diplocraterion* isp. preserved on thin-bedded carbonate mudstone, bed 42, SSK; G, *Megagrapton irregulare*, bed 42, DWZ.

Fig. 5. Field photos showing trace fossils from the Middle Triassic Guanling Formation. A, *Palaeophycus,* bed 172, XDP; B, *Planolites*, bed 171, SSK; C, *Rhizocorallium* isp.; bed 168, XDP; D, *Rhizocorallium commune*, bed 71, XDP. E, *Rhizocorallium commune,* bed 70, DWZ. F, detail showing the faecal pellets in marginal tubes of *R. commune.* G, *Sinusichnus* isp.*,* bed 40, XDP. Note the Y-shaped (white arrow) and T-shaped (black arrow) branchings in burrow system. H is a sketch of G showing the overall morphology of *S.* isp..

Fig. 6. Field photos showing trace fossils from the Middle Triassic Guanling Formation. A, *Spongeliomorpha* isp., bed 9 SSK. Note the longitudinal scratch marks on burrow surface (white arrows). B, *Taenidium barretti*, bed 35, SSK; C, *Thalassinoides suevicus*, bed 34, SSK. Note the swelling and Y-shaped branching in *Thalassinoides suevicus* (arrows). D, *Undichna unisulca*, Bed 105, DWZ; E, *Zoophycos* isp. ?; Guangling Formation, Boyun; F, *Zoophycos* isp., DWZ; Coin is 2.5 cm in diameter, DWZ.

Fig. 7. Burrow size measurements of commonly occurring trace fossils at Luoping, Yunnan Province. A, *Planolites*, bed 171, XDP; B, large sized *Rhizocorallium commune*, isp., bed 36, XDP; C, small sized *Rhizocorallium* isp., bed 168, XDP; D, *Thalassinoides suevicus*, Bed 34, SSK.

Fig. 8. Statistical analysis of pyrite framboids from fossil beds of the Luoping Biota. A, SEM photo showing pyrite framboids from marly carbonate mudstone, bed 15, SSK section. Note the abundant pyrite framboids (black arrows) of similar sizes occurring densely. B, Histogram showing the distribution of diameters of pyrite framboids for rock samples from the same bed. C, SEM photo of framboid pyrite from carbonate mudstone, bed 33, SSK. D, Histogram showing the diameter distribution of pyrite framboids for rock samples of the same bed MD = mean diameter; SD = standard deviation.

Fig. 9. Burrow size comparison of typical ichnotaxa from latest Permian to Middle Triassic. A, *Planolites*; B, *Rhizocorallium*; C. *Thalassinoides*; Changh.: Changhsingian; Grie.: Griesbachian; Die.: Dienerian.

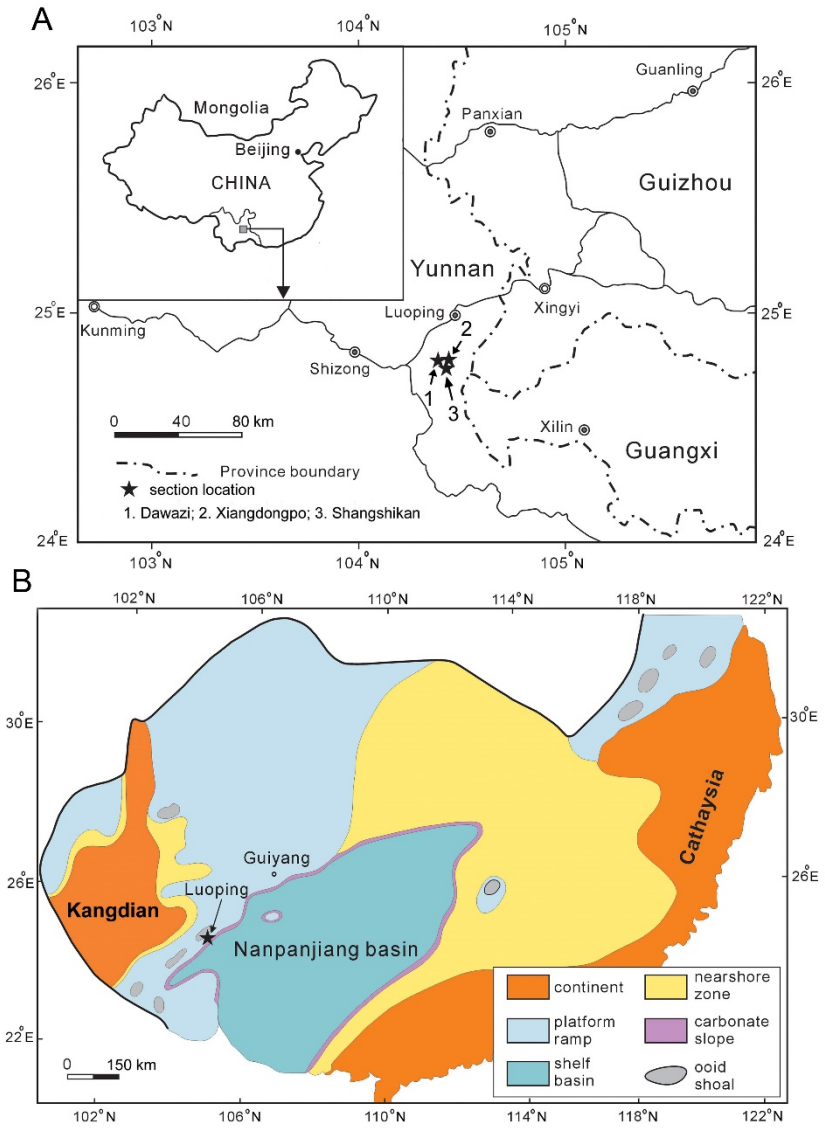
A
103°N
104°N
105°N
26°E
25°E
24°E
Mongolia
Beijing
CHINA
Guanling
Panxian
Guizhou
Yunnan
Luoping
Xingyi
Kunming
Shizong
1
2
3
0 40 80 km
Province boundary
section location
1. Dawazi; 2. Xiangdongpo; 3. Shangshikan
Xilin
Guangxi
B
102°N
106°N
110°N
114°N
118°N
122°N
30°E
26°E
22°E
Cathaysia
Guiyang
Luoping
Kangdian
Nanpanjiang basin
0 150 km
continent
nearshore zone
platform ramp
carbonate slope
shelf basin
ooid shoal

Figure 1

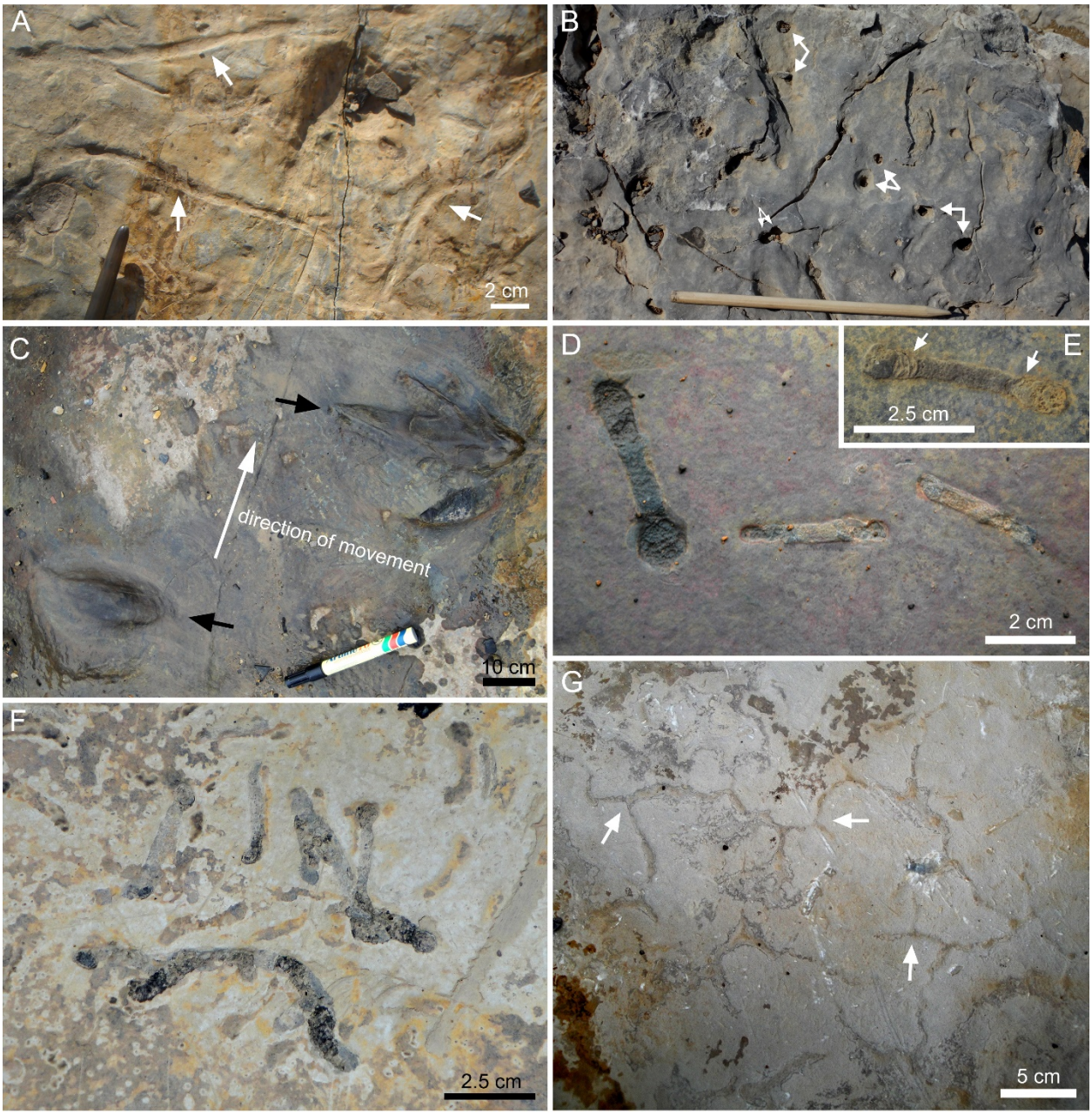

Figure 4

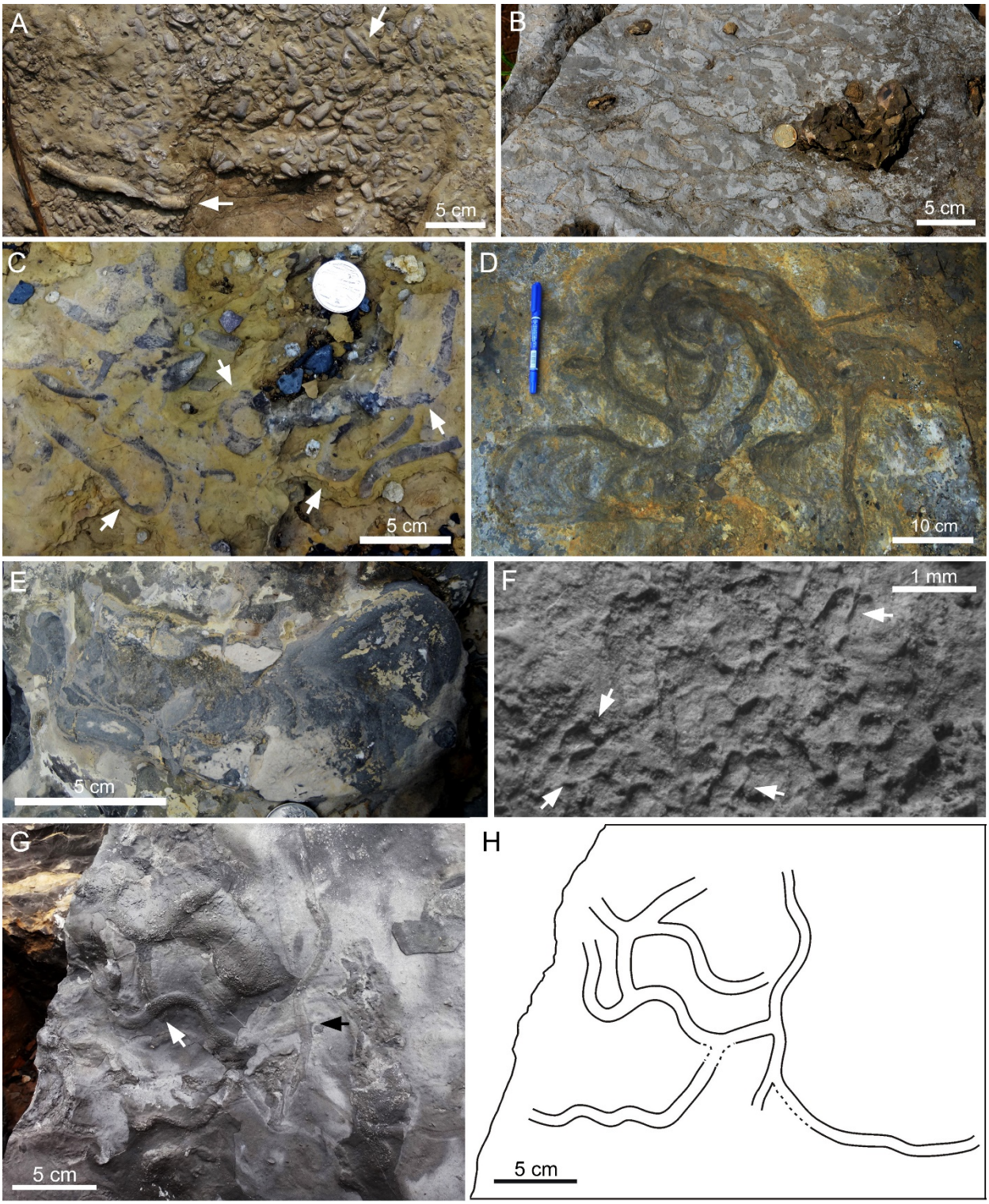

1233

1234 **Figure 5**

1235

1236

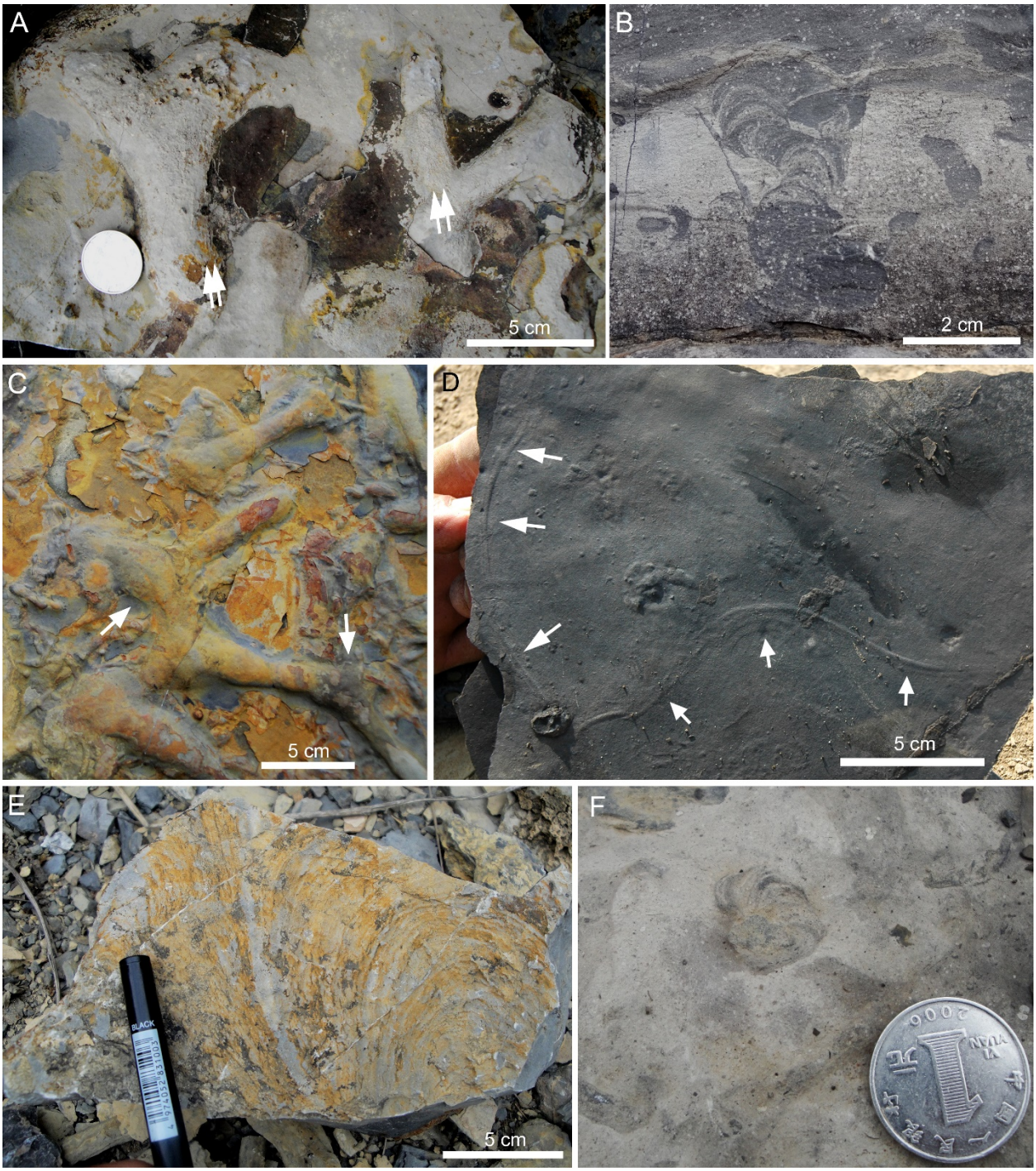

1237

1238 **Figure 6**

1239

1240